



Estimating the inventory of volatile gases in a BWR reactor using OpenMC

Bachelor thesis

Student: Eliise Kaha

Student code: 206093YAFB

Supervisor: Marti Jeltsov, PhD, Research Fellow KBF1; Hando Tohver, MSc, Junior Research Fellow

UT

Study program: Applied Physics, YAFB02/2



Lenduvate gaaside inventari hindamine keevaveereaktoris kasutades OpenMC-d

Bakalaureusetöö

Üliõpilane: Eliise Kaha

Üliõpilaskood: 206093YAFB

Juhendaja: Marti Jeltsov, Phd, Teadur KBFI; Hando Tohver, MSc, Nooremteadur UT

Õppekava: Rakendusfüüsika, YAFB02/2

Declaration

Hereby I declare that I have compiled the paper independently and all works, important standpoints and data by other authors have been properly referenced and the same paper has not been previously presented for grading.

Author: Eliise Kaha

The paper conforms to requirements in force.

Supervisor: Marti Jeltsov, Hando Tohver

Permitted to the defence.

Chairman of the Defence Committee: Vladislav-Veniamin Pustõnski

Contents

Declaration	3
1 Abbreviations	6
2 Introduction and problem description	7
3 Theoretical Basis	9
3.1 What are Light Water Reactors and Boiling Water Reactors?	9
3.2 What is fission process and burn-up?	10
3.3 What is nuclear fuel?	11
3.3.1 What is spent nuclear fuel?	11
3.3.2 What are BWR design specifics?	12
3.4 Which volatile gases are present in spent nuclear fuel?	13
3.5 What is Monte Carlo Simulation?	14
3.5.1 How is Monte Carlo Simulation used for Neutron Transport?	14
3.6 What is OpenMC?	15
3.6.1 What is depletion analysis and how can depletion analysis be done with OpenMC?	15
4 Implementation	19
4.1 Which depletion chain files were used?	20
4.2 What model was used for depletion analyses?	20
5 Results on volatile gases inventory	22
5.1 Model validation and initial analyses	22
5.2 ^{129}I production according to burn-up and void fraction	24
5.3 ^{14}C production according to burn-up and void fraction	26
5.4 ^3H production according to burn-up and void fraction	27
5.5 ^{85}Kr production according to burn-up and void fraction	29
5.6 Volatile gases	31
5.7 Discussion and conclusions	32

5.8	Further research	33
6	Abstract	34
7	Annotatsioon	35
	Acknowledgements	36
8	References	37
9	Appendix	41
9.1	Appendix 1. Depletion file creation modified code	41
9.2	Appendix 2. Fission yields file formatting code	42
9.3	Appendix 3. Material definition formatting example	43
9.4	Appendix 4. Volume data extraction code example	43
9.5	Appendix 5. Phase III-C benchmark results for 40% void	44
9.6	Appendix 6. Phase III-C benchmark results for 70% void	45
9.7	Appendix 7. Mass data extraction code example	46
9.8	Appendix 8. Source term STEP-3 fuel assembly.....	47
9.9	Appendix 9. Non-exclusive licence for reproduction and publication of a graduation thesis	48

1 Abbreviations

BWR – Boiling Water Reactor

CAD – Computer-Aided Design

ENDF –Evaluated Nuclear Data File

FANT – Faunte Ampliada de Neutrones Termicos

GEH – General Electric Hitachi

GWd/tHM – gigawatt-days per metric ton of heavy metal

HDF – Hierarchical Data Format

JEFF – The Joint Evaluated Fission and Fusion File

LWR – Light Water Reactor

NEA – Nuclear Energy Agency

NPP – Nuclear Power Plant

PWR – Pressurised Water Reactor

SMR – Small Modular Reactor

STEP – Spherical Tokamak for Energy Production

2 Introduction and problem description

The main objective of this thesis is to estimate the inventory of volatile gases in reference to BWR fuel assemblies. Volatile gas production in reactor fuel becomes of utmost importance during severe accidents. When the protective barriers separating the irradiated fuel from the environment are compromised, there is a potential for the isotopes produced within the fuel to escape into the surrounding environment. In this case knowing the concentration of volatile gases is crucial to ensure the safety of nuclear plant workers and civilians alike. The risk is high with long-lived volatile gases, which have the necessary time to spread all over the world. Fission reaction produces many volatile isotopes but from a long-term safety point of view, four are critical: Iodine-129 (^{129}I , half-life $1.7 \cdot 10^7$ years), Tritium (^3H , half-life 12.2 years), Krypton-85 (^{85}Kr , half-life 10.73 years) and Carbon-14 (^{14}C , half-life 5730 years) [1]. These four volatile gases will be thoroughly analysed in this thesis.

NPP safety has always been a heavily talked about topic, even more so after the 2011 accident in the Fukushima Daiichi Nuclear Power Station [2]. During the decommissioning of Fukushima Daiichi Nuclear Power Station, one of the key issues has been the criticality control of damaged nuclear fuel [2]. In order to evaluate criticality parameters of the mixture of damaged fuel with other materials the average isotopic composition of spent nuclear fuel, as a function of burn-up, is required [2]. For this reason, an international burn-up calculation benchmark Phase III-C benchmark was created. In this thesis, the benchmark is used to evaluate the volatile gas inventory modelling instead of criticality per se. The geometry for BWR assembly in this thesis matches the one described in the benchmark.

Determining the isotopic composition of spent fuel is complicated. Physical experiments are expensive and dangerous to conduct due to the high levels of ionizing radiation released from the irradiated fuel. Computer modelling is often used as an economic and safe alternative. The Monte Carlo method is the most commonly used algorithm for nuclear data analysis on existing and new nuclear systems. Due to the strategical value of Monte Carlo codes, in the field of nuclear energy, most software is export-restricted and not easily accessible. During recent years, open-source codes such as OpenMC have been gaining popularity due to their flexibility and open-collaboration approach [3].

This study was conducted using OpenMC. By default, OpenMC does not support the estimation of light volatile isotopes that are created during ternary fission events as it recommends ENDF/B-VII.1 and ENDF/B-VIII.0 nuclear data library for depletion (U^{235} depleting into different isotopes during fission processes) analyses [4, 5, 6]. One of the tasks of this thesis was to implement the missing interaction data such that these evaluations would become possible. Using existing nuclear data libraries, a new depletion chain file was created describing all volatile isotope transmutations and decay channels. This approach will make it possible to represent the missing volatile isotope transmutations in future case studies.

This thesis uses OpenMC capabilities to conduct depletion analyses using the Monte Carlo Method on a BWR reactor assembly model after Phase III-C benchmark. Volatiles production is simulated as a function of burn-up during power plant operation throughout fuel life cycle. Fuel life cycle starts from approximately 0 GWd/tHM and ends at approximately 50 GWd/tHM. Afterwards, the fuel will be removed from the reactor and is considered spent nuclear fuel. Spent nuclear fuel isotopic composition is critical for nuclear accident damage control as well as nuclear waste storage purposes.

The main objective of this thesis is estimating the evolution of four long-lived volatile gases ^{129}I , ^{14}C , ^3H , ^{85}Kr inventory over fuel lifetime in a BWR using OpenMC capabilities. For this purpose, depletion analyses of BWR fuel assembly will be done with OpenMC, which uses Monte Carlo method to calculate the path of each particle. This analysis gives an overview of nuclide production in nuclear fuel throughout BWR operation.

3 Theoretical Basis

3.1 What are Light Water Reactors and Boiling Water Reactors?

Most nuclear power plants used today are Light Water Reactors (LWR) [7]. LWRs are similar to other types of conventional thermal power plants, the only difference being nuclear reactions heating up water, which is converted to steam and passed through steam turbines for electricity [7]. Initially, LWRs were primarily used on submarines, where Pressurised Water Reactors (PWRs) were preferred [8]. PWRs have two cycles of water: the first containing the core, isolating the primary coolant from the secondary cycle [7]. The primary coolant is passed through a heat exchanger, which heats the water in the secondary cycle until boiling [7]. The steam then moves to the turbine, which starts turning and, in turn, drives the generator for electricity creation. PWRs use a pressurizer to keep the water in the first cycle in a liquid state [7]. PWRs were preferred for submarine maintenance and non-contaminated space optimization [8].

Once nuclear power plants started to be used for large-scale energy production, Boiling Water Reactors (BWRs) started gaining popularity [8]. The first experimental boiling water reactor was built in 1942 at the Argonne National Laboratory in Chicago, Illinois [9]. In commercial use, the water boils directly in the reactor pressure vessel making the second (non-radioactive) cycle unnecessary, hence the popularisation of BWRs [8]. In a BWR, the coolant water flows into the core where it is boiled, and the mildly radioactive steam moves straight to the turbine, which starts turning, thereby driving the generator to produce electricity that can be directed to the grid or used for auxiliary consumption [7]. The radioactivity in the steam is a byproduct of fission processes happening inside reactor vessel.

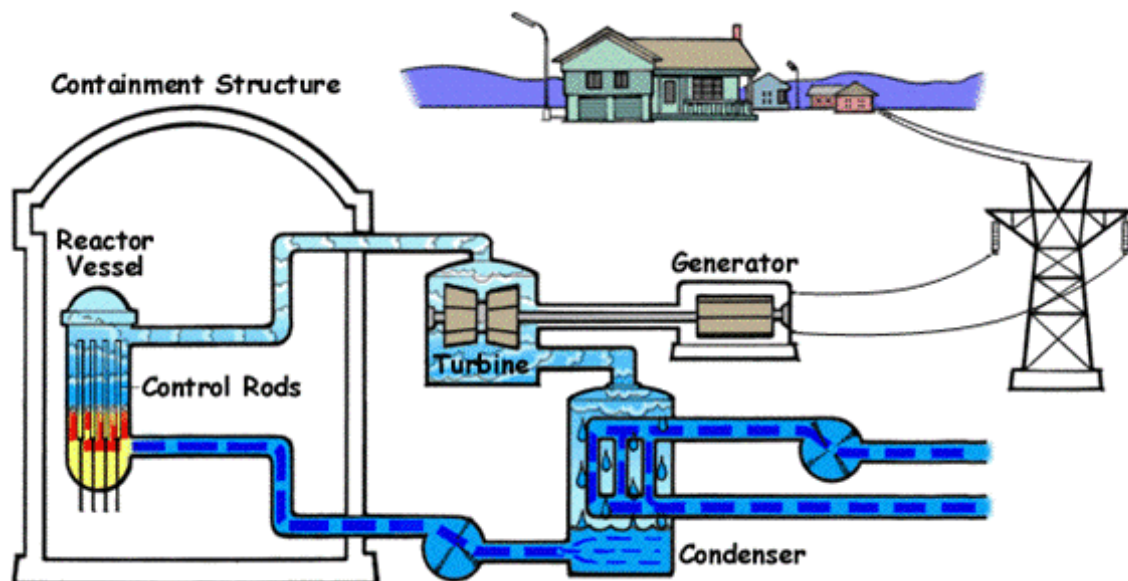
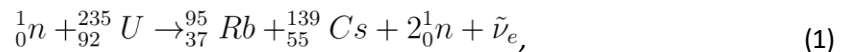


Figure 1: Schematic of a boiling water reactor [9]

3.2 What is fission process and burn-up?

The fission process can be described as nucleus splitting into fragments following neutron absorption [10]. If the nucleus divides into two fragments, the process is called binary fission, and if it divides into three, it is referred to as ternary fission [10]. Typically, binary fission does not result in two same mass particles, but one is a bit heavier than the other. For U-235, one example of binary fission reaction is



where 1_0n refers to a neutron, ${}^{235}_{92}\text{U}$ to the uranium isotope with the atomic mass of 235, 143 neutrons and 92 protons in the nucleus, Rb to the rubidium isotope with the atomic mass of 95, 58 neutrons and 37 protons in the nucleus, Cs to the Caesium isotope with the atomic mass of 139, 84 neutrons and 55 protons in the nucleus, and $\tilde{\nu}_e$ to the released neutrino [10]. Fission products are usually neutron heavy isotopes [10]. In Figure 2, it is shown how fission produces products with various mass numbers. The most probable fragment masses are around mass 95, which correspond to Krypton-95, and 137, which correspond to Barium-137 [11].

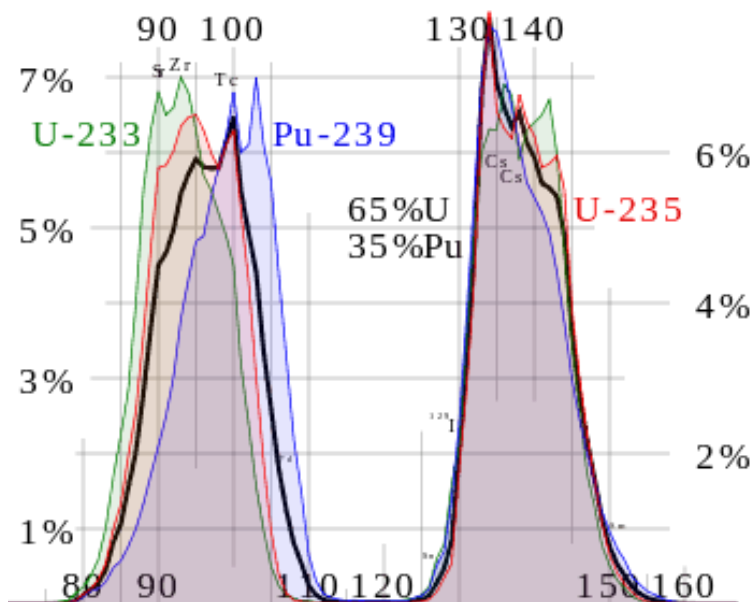


Figure 2: Fission fragment yield for different nuclei [11]

The energy released per unit mass of uranium is called fuel burn-up. Burn-up is described using various units, most commonly the energy is given in gigawatt-days and mass corresponds to the initial heavy metal content in fuel (metric ton). Fuel burn-up can also be defined as energy extracted from the fuel [12]. Therefore, it describes the fission energy release per unit mass of fuel in gigawatt-days per metric ton of heavy metal of uranium (GWd/tHM) [13].

3.3 What is nuclear fuel?

Nuclear fuel in most commercial reactors is made up of ceramic pellets containing enriched uranium dioxide, which can be seen in Figure 3. Uranium enrichment involves increasing the proportion of uranium-235 in natural uranium before using it to create ceramic pellets for use in reactors. These pellets are stacked vertically into fuel rods, generally made of zirconium alloys. Fuel rods are bundled together to create fuel assemblies, which can be seen on Figure 4. Fuel assemblies



Figure 3: Pressed pellets of uranium dioxide [53]



Figure 4: Fuel assembly [53]

will eventually be placed into the reactor core in a structured configuration. Fuel is solid going in and will remain as such when it comes out. Nuclear fuel that has been removed from the reactor is called spent nuclear fuel. [14, 15]

3.3.1 What is spent nuclear fuel?

When nuclear fuel has been used in a nuclear reactor for about five years, it will be removed from the reactor and becomes spent nuclear fuel [16]. After this initial five-year period, more than 90% of the potential energy remains in the fuel [14]. Such fuel is recyclable, and some countries like France do recycle the spent fuel to be used again (extracting unused uranium and plutonium). There are some reactor designs in development that could even reuse today's spent fuel without any modifications as nuclear fuel [14]. The whole nuclear fuel cycle can be seen in Figure 5.

The fuel life cycle inside the reactor is described by different values of fuel burn-up. All factors of fuel composition are also dependent on fuel pin positions in the core, meaning fuel assembly burn-up is determined as an average over pin burn-up rates in that assembly [12]. The maximum burn-up a fuel assembly can achieve is dependent on the power history, reactor design and operation strategy. The average discharge fuel burn-up has increased in time, the modern LWR fuel discharge can range from the average 45 GWd/tHM to 55 GWd/tHM [17, 18]. Current average fuel burn-ups considered for BWR is 50 GWd/tHM or even higher [18]. Depending on the rod placement, burn-up of the individual rods can differ as initial enrichment in fuel rods can be different and boiling is usually not homogeneous.



Figure 5: Nuclear fuel cycle, process starting from uranium mining and ending with nuclear waste disposal [15]

The radioactivity of spent nuclear fuel is gained during nuclear reactor operational years, as nuclear reactions take place throughout the core and new, non-stable or in other words radioactive elements are created. Radioactivity is the phenomenon of unstable nuclei disintegrating spontaneously into more stable nuclei [19]. Knowing the numeric concentration of isotopes in spent fuel, the radioactivity can be calculated with the following:

$$R = \lambda \cdot N \quad (2)$$

where

$$\lambda = \frac{\ln(2)}{T_{\frac{1}{2}}} \quad (3)$$

and

$$N = \frac{m}{M} \cdot N_A \quad (4)$$

In these formulas R is rate of radioactive decay, λ is the decay constant/branching ratio, N is the number of radioactive atoms present. $T_{1/2}$ is the nuclei half-life, M is the molar mass, m is the mass and N_A is Avogadro's number ($\sim 6.022 \cdot 10^{23}$).

3.3.2 What are BWR design specifics?

BWR fuel assemblies used to contain 8x8 rods [7], however 9x9 fuel assemblies have gained popularity in newer designs [2]. There are about 400-700 fuel assemblies in the core of a large BWR [7]. One of the more known BWRs are The Fukushima Daiichi reactors, which are GE boiling water reactors and had 400 fuel assemblies in unit 1, 548 in units 2-5, and 764 in unit 6. Each fuel assembly contained 60 fuel rods, meaning 8x8 rods in a nuclear fuel assembly [20]. The fuel rod cladding is made of low neutron absorbing zirconium alloy, that holds uranium oxide fuel in it. Reactor power

in the Fukushima Daiichi reactors all together is 4696 MW, unit 1 possesses the power of 460 MW, units 2-5 784 MW, unit 6 764 MW [20].

In Estonia another GE Hitachi BWR design has gotten more recognition. BWRX-300 is a 300 MW Small Modular Reactor (SMR). GE Hitachi Nuclear Energy's (GEH's) BWRX-300 is the most modern GE Hitachi nuclear reactor, which has been designed-to-cost, meaning the cost of the product is predetermined during the design phase. BWRX-300 has 240 fuel assemblies, which have 10x10 fuel rods. [21]

NPP size and configuration of fuel assembly are not the only defining characteristics of a BWR. For a BWR to achieve the high burn-up of 50 GWd/tHM, reactor power control methods are necessary. One of those methods is the use of special burnable poisons in the fuel rods. In some BWR-s gadolinium oxide is used as the burnable poison. [22, 23]

3.4 Which volatile gases are present in spent nuclear fuel?

During the operational years of a nuclear power plant nuclear fuel depletes and various nuclear reactions produce volatile gases, which are elements that easily evaporate at room temperature (20 °C). Fission reactions create many volatile isotopes. Four of them are critical from a safety point of view: Iodine-129 (I-129), Tritium (H-3), Krypton-85 (Kr-85), and Carbon-14 (C-14) [1].

I-129 appears as a fission product or as a radioactive decay product of Tellurium-129 (Te-129), Antimony-129 (Sb-129), or Tin-129 (Sn-129), which are short-lived fission products [24]. I-129 itself has a long half-life of $1.7 \cdot 10^7$ years and because of that is a useful isotope to trace for studying transport processes in environment [25, 24]. Furthermore I-129 is an important isotope to consider in studies since it's thought to be one of the main radioactive dose providers from nuclear waste disposal sites into biosphere [26]. When it eventually decays, it becomes the stable isotope Xenon-129 [24]. Iodine-129's fission yield is about 0.67% to 1.77 %, meaning about 0.67% to 1.77 % of U-235 fission reactions end in I-129 [27].

Compared to I-129, Tritium has a short half-life of only 12.2 years, though it is still considered relatively long, as it is sufficient for the volatile tritium to be distributed all over the world [24, 28]. It decays into stable isotope Helium-3 [24]. In light water reactors, Tritium is mainly formed by ternary fission of uranium, where instead of two fission products there are three [24, 1]. In rarer cases it is produced by neutron activation of lighter hydrogen isotopes [1]. In the environment, Tritium is considered a mobile isotope and has a long half-life, therefore, careful deliberation must be put behind its waste management [28]. Tritium's fission yield is about 0.01% to 0.03 %, meaning 0.01% to 0.03 % of U-235 fission reactions end in Tritium [27].

Krypton-85 is generated through the fission of U-235, a process prevalent in nuclear fuel. Kr-85 has a half-life of 10.73 years and decays to the stable isotope rubidium-85 [24]. In today's practice most Kr-85 produced in NPPs is released uninterrupted into the environment from off-gas stacks, which considering Kr-85 is a long-lived isotope can be a sizable environmental impact depending on how

much Kr-85 is produced during NPPs operating [1]. This practice is used, because Kr-85 is a noble gas, which does not interact with surrounding environment and dilutes quickly in the environment [1]. Krypton-85's fission yield is about 0.26% to 0.57 %, meaning about 0.26% to 0.57% of U-235 fission reactions end in Kr-85 [27].

Carbon-14 decays to the stable isotope nitrogen-14 after a half-life of 5730 years [24]. In the reactor core, C-14 is present after neutron reaction with N-14, N-15, O-16, O-17. Additionally, there is a small chance of C-14 appearing when C-13 absorbs a neutron. C-14 is widely produced, as nitrogen is present in the fuel gaps and reactor coolant as an impurity, and oxygen is a significant component of oxides used in Light Water Reactors [24, 28]. Carbon-14 is easily transported through biological processes and in the human body it behaves as ordinary carbon [28]. C-14 half-life in a human body is ~40 days, in that time inhaled $^{14}\text{CO}_2$ can be transported from the lungs all over the body [28]. This makes C-14 a mobile isotope with a long half-life, for which waste management is considerably harder than some highly radioactive short-lived isotopes [28].

3.5 What is Monte Carlo Simulation?

Monte Carlo Simulation, more commonly known as the Monte Carlo method, is a computer based mathematical method that uses random sampling to find probable numerical values for arbitrary events [29]. Over the years it has been successfully used for many scientific problems [30]. Today, Monte Carlo method is widely used in different areas of life: video games, stock market analysis, sales forecasting, project management, and the hottest topic in today's society: artificial intelligence.

Monte Carlo method was created by Stanislaw Ulam and John von Neumann, who both worked on the Manhattan Project at Los Alamos [31]. Stanislaw Ulam came up with the idea of Monte Carlo method from an interest in wanting to know how big the chance of winning Solitaire is [30]. He later introduced his idea to John von Neumann, with whom they began planning the actual algorithm [30].

3.5.1 How is Monte Carlo Simulation used for Neutron Transport?

Thinking of the Monte Carlo method for neutron transport, the first logical conclusion might be that in order to determine the result, the neutron transport equation has to be solved [32, 33]. The neutron transport equation, also called Boltzmann transport equation, is:

$$\begin{aligned} & \frac{1}{v} \frac{\partial \phi}{\partial t} + \frac{\partial \phi}{\partial x} + \Sigma_t \phi(x, E, t) \\ = & \int_0^\infty \int_{4\pi} \Sigma_s(E' \rightarrow E, \Omega' \cdot \Omega) \phi(x, E', \Omega', t) d\Omega' dE' + S(x, E, \Omega, t) \end{aligned} \quad (5)$$

where $\varphi(x,E,\Omega,t)$ is the neutron flux, representing the number of neutrons per unit area, per unit time, per unit energy, and per unit solid angle, v is the neutron speed, Σ_t is the total macroscopic cross-section, representing the probability of a neutron interacting per unit path length, $\Sigma_s(E' \rightarrow E, \Omega' \cdot \Omega)$ is the scattering macroscopic cross-section, representing the probability of a neutron scattering from energy E' and direction Ω' to energy E and direction Ω , and $S(x,E,\Omega,t)$ is the external neutron source term. Neutron transport equation cannot be solved analytically, however with many simplifications the equation can be solved deterministically.

Like the deterministic calculation, The Monte Carlo stochastic calculation for neutron transport is also based on the neutron transport equation [34, 32]. However rather than solving a huge set of algebraic equations the transport of individual particles is simulated according to the equation [34, 32]. The average behaviour of the particles in a real system from the average behaviour of the simulated particles gives the result [34, 32]. For each neutron, a series of probabilistic events that describe the interactions with matter are simulated [33]. These event histories are tracked to determine a probability distribution that characterizes the physical phenomena of neutron reactions [33].

Histories start from user-defined source locations or fission sites and end at the neutron absorption or leakage site. The results of the simulation conclude from a large number of those individually simulated neutron histories. The Monte Carlo method is capable of calculating statistical estimates for reaction rates without solving the flux distribution. Therefore, it gives the user the ability to use bigger variations in space and energy variables. [33]

3.6 What is OpenMC?

OpenMC is a simulation code that uses the Monte Carlo method for neutron and photon transport. For models built using either constructive solid geometry or CAD representation, OpenMC is capable of performing fixed source, k-eigenvalue, and subcritical multiplication calculations. Using OpenMC, it is possible to use both continuous energy and multigroup transport. When using continuous-energy particles, the interaction data is produced in HDF5 format. [3]

3.6.1 What is depletion analysis and how can depletion analysis be done with OpenMC?

In the nuclear fuel context depletion means ^{235}U depleting into different isotopes. There are many codes using Monte Carlo Method, that have the ability to simulate fuel depletion in an NPP. These codes depletion analysis estimate the burn-up and the concentration of isotopes in the fuel [35]. For this theses the depletion analysis will be done with OpenMC, which uses Monte Carlo method to simulate fuel depletion.

For depletion calculations with OpenMC we need to use nuclear data libraries, that provide isotopes with cross sections, neutron-induced fission yield data and decay data. In this thesis we will use 3

different libraries: ENDF/B-VII.1, ENDF/B-VIII.0, JEFF-3.3. For depletion analysis in OpenMC, a file describing the depletion chain is needed. This chain describes transmutation and decay reactions, which result in the change of isotope concentrations over time [36]. Pre-generated depletion chains exist for ENDF/B libraries. Unfortunately, some of the volatile gases are partially described in these libraries, as ternary fission paths do not exist in the data. This makes the libraries underestimate ^{14}C and ^3H production. A new depletion file, using nuclear data from the JEFF-3.3 library, was created for this thesis, to have accurate results for all four long-lived volatile gases. All three aforementioned nuclear data libraries use ENDF nuclear data library formatting.

3.6.1.1 What are ENDF nuclear data libraries?

ENDF libraries are collections of material evaluated by a recognized evaluation group, stored in a computer-readable format. Libraries can be used as an input of nuclear data to a neutron calculation model. The ENDF systems are used in many nuclear data applications, where pre-evaluated nuclear data might be necessary. The ENDF system comprised of procedures and formats, meaning:

- rules of what data needs to be included in what format and descriptions of how the data is arranged in libraries,
- formulas for the reconstruction of physical quantities such as cross sections and angular distributions. [37]

In this thesis, the ENDF-6 format was used, with 6 indicating how the data in this specific file was tabulated and how the processing code must read it [37]. More specifically, three versions of libraries with the ENDF-6 format were analysed, from two recognized evaluation groups. From JEFF - NEA Joint Evaluated Fission and Fusion Files version JEFF3.3 was used, and from ENDF/B - United States Evaluated Nuclear Data Files versions ENDF/B-VII.1 and ENDF/B-VIII.0 were used.

3.6.1.2 What are ENDF/B-VII.1, ENDF/B-VIII.0 libraries?

United States Evaluated Nuclear Data File (ENDF/B) is maintained by National Nuclear Data Center (NNDC). New versions of ENDF/B nuclear data libraries are all extensively reviewed and tested, which makes them a standard reference data during the library's lifetime [37]. All ENDF/B nuclear data libraries contain recommended assessments for materials, which are as complete as possible. However, the data completeness is dependent on the intended use and no library can accommodate all different nuclear data analyses [37]. In reference to these theses ENDF/B libraries are missing ternary fission, which makes these libraries less ideal for describing production of volatile gases: ^{14}C and ^3H .

ENDF/B-VII.1 released December 22, 2011 is built on ENDF/B-VII.0 by improving many aspects. All 229 evaluations in ENDF/B-VII.0 were updated and 20 were added to the ENDF/B-VII.1 assemble. However, only the neutron, fission product yield, and decay data sub-libraries were modified. Meaning ENDF/B-VII.0 standard evaluation stayed unchanged. [38]

ENDF/B-VIII.0 released on February 2, 2018 was assembled by Cross Section Evaluation Working Group (CSEWG), they incorporated work from all over US and international nuclear science community into ENDF/B-VIII.0. IAEA standard includes the improvements made from older ENDF/B-VII.1 into ENDF/B-VIII.0. ENDF/B-VII.1 performed generally well in validation tests. However, ENDF/B-VIII.0 has many upgrades to important nuclides. [4]

3.6.1.3 What is JEFF-3.3 library?

The Joint Evaluated Fission and Fusion File (JEFF) is an evaluated library produced via international collaboration of Nuclear Energy Agency (NEA) Data Bank participating countries, originally released in November 1992. The library has been updated on multiple occasions, with JEFF-3.3 being the latest version released in 2017. It includes a thorough update of neutron, decay data, fission yields, dpa, and neutron activation libraries in the EAF format, with neutron thermal scattering files for 20 compounds. Additionally, it includes special sub-libraries for incident alphas, deuterons, gammas, helium-3, protons, and tritons, which have been contributed by the TENDL-2017 library and were adopted as part of JEFF-3.3. [39, 40]

In this study Neutron, Decay Data, and Fission Yields files in ENDF-6 format were used from the JEFF-3.3 library to create a depletion chain file capable of estimating the inventory of volatile gases. For this purpose, an existing code [41] (used to create a depletion chain file from ENDF-B-VII.1 files) was modified to use JEFF-3.3 files.

3.6.1.4 Is there a difference in using Nuclear Data Libraries ENDF/B and JEFF?

Different versions of ENDF/B and JEFF libraries have been compared many times for research purposes. “Comparison of FANT results using the ENDF/B-VII.1, JEFF-3.3 and TENDL 2017 nuclear libraries” [42] was published in 2020. The paper’s main goal was to compare three widely used nuclear data libraries: JEFF-3.3, ENDF/B-VIII.1, and TENDL2017. They were compared in a material activation device called FANT¹ by neutron irradiation² locating the neutron spectrum in this device mainly in the thermal range. In this research the author deducted no significant differences in results while calculating with the three different libraries using Monte Carlo method. Nevertheless, the author made observations about the libraries. Comparing the libraries to experimental results, the author realized that the JEFF-3.3 nuclear data library gave the most accurate results, while the ENDF/B-VII.1 library had a tendency to underestimate.

¹ FANT (Faunte Ampliada de Neutrones Termicos; in Spanish) is a thermal neutron irradiation facility with an extended and very uniform irradiation area, that has been developed by the Neutron Measurements Laboratory of the Energy Engineering Department at Universidad Politecnica de Madrid (LMN-UMP). [42]

² Neutron irradiation of structural materials results in the production of a variety of atomic – size defects, which generally increase the strength and can severely reduce ductility. [54]

In a research paper titled “Comparison of the ENDF/B-VII.0, ENDF/B-VII.1, ENDF/B-VIII.0 and JEFF-3.3 Libraries for the Nuclear Design Calculations of the NPP Krško with the CORD-2 System” [43] an assessment of the impact that nuclear cross-section libraries have on calculations of the Krško NPP nuclear core was conducted. Calculations were performed on a single fuel assembly in an infinite array. The results showed a difference in multiplication factor in fresh fuel. This phenomenon was caused by the difference in U-235 neutron cross-section in the libraries. Burned fuel also showed a difference, which was caused by unequal rates for Pu production. Core critical boron concentration measurements indicated elevated boron levels using the nuclear data libraries ENDF/B-VII.0, ENDF/B-VIII.0, and ENDF/B-VII.1. Isothermal coefficients by cycle 30 were elevated for the libraries JEFF-3.3 and ENDF/B-VIII.0.

A validation of the JEFF-3.3 nuclear data library has been done for ANSWERS code in a research paper called “Validation of JEFF-3.3 and ENDF/B-VIII.0 nuclear data libraries in ANSWERS codes” [44]. For this, the authors produced new continuous energy (BINGO) and multi-group (WIMS) nuclear data libraries based on JEFF-3.3 and ENDF/B-VIII.0 for the ANSWERS Monte Carlo code MONK and the deterministic code WIMS. Then, the calculations done with the generated files were compared to calculations with existing files that were based on nuclear data libraries JEFF-3.1.2 and ENDF/B-VII.1. The authors concluded that all evaluations performed adeptly against experiments, yet some were better than others under specific circumstances. This fact demonstrated the need for nuclear data library users to validate their cases against comparable references. As a result, the authors recognize that in some cases JEFF-3.3 produces improved agreement with experiments. Comparison of nuclear data libraries ENDF/B and JEFF shows that both evaluated libraries are useful for different analyses. In this thesis ENDF/B-VII.1, ENDF/B-VIII.0 and JEFF-3.3 will be used as all have their benefits.

3.6.1.5 How are the nuclei data stored?

In this thesis, we need to store a lot of data about nuclei. For this purpose, we use the Hierarchical Data Format i.e., the H5 format. This kind of file stores a large amount of data in the form of multidimensional arrays [45]. The attributes in the H5 file for nuclei include the filetype, version, energy groups, delayed groups (if applicable), the group structure defining the boundaries and cross-section data [46]. Cross-section data inside the file is categorized under temperature-dependant multi-group data, temperature dependant data and temperature dependant neutron scattering data [46].

The section temperature-dependant multi-group can describe: the atomic weight ratio, whether the dataset is fissionable and the representation method for cross sections, scattering properties. Temperature-dependent data is structured under sections defined by temperature in Kelvin. Under the section there can be cross-section data: total, absorption, fission, kappa-fission, chi, nu-fission, and inverse-velocity. Temperature dependant neutron scattering data can contain details on the minimum and maximum energy groups with non-zero values of the scattering matrix, as well as flattened representations of the scattering moment and multiplicity matrices. [46]

4 Implementation

The implementation process started with setting up the Docker software and OpenMC. The process ended with visualizing the results. The whole process is demonstrated in Figure 6.

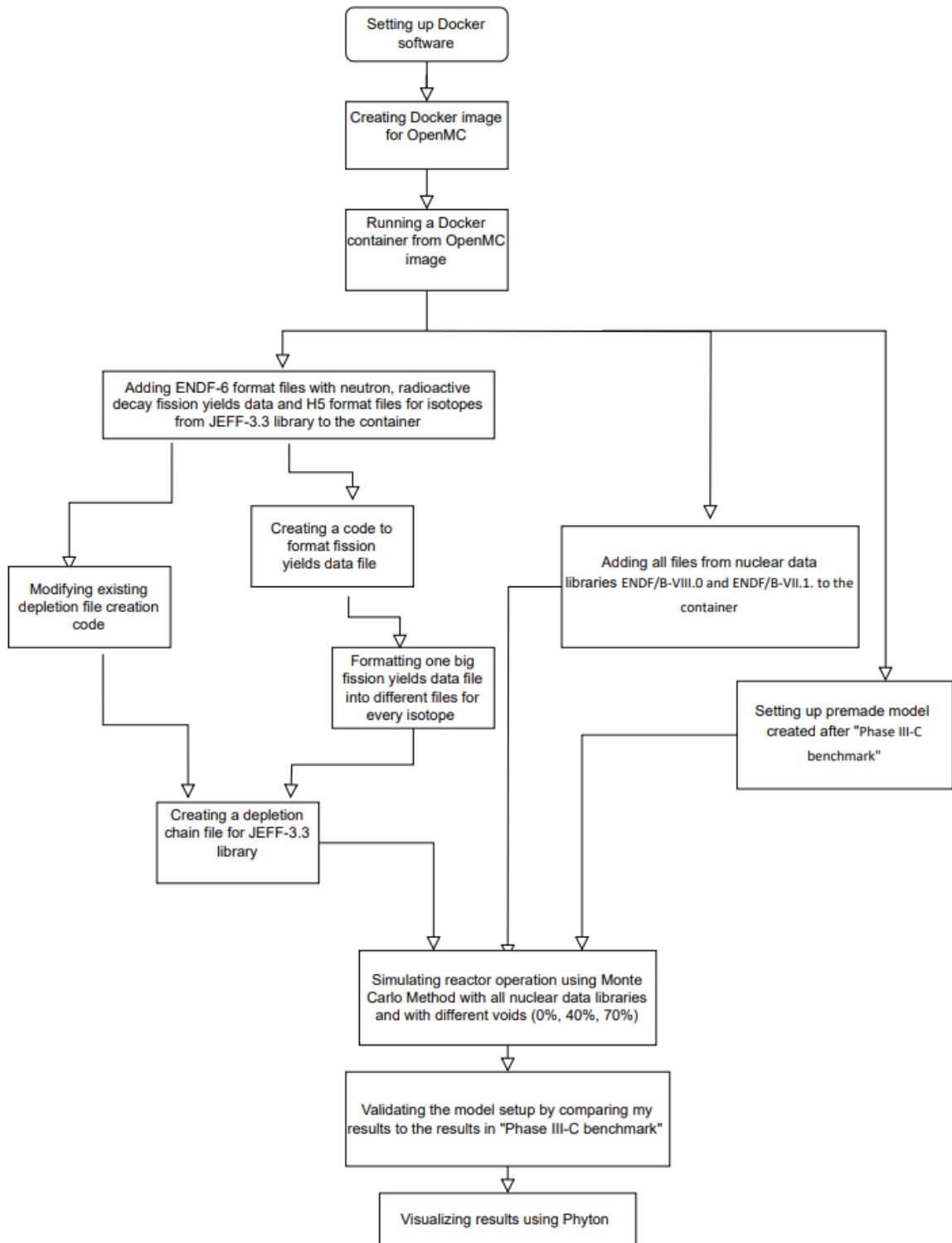


Figure 6: Visualization of implementation process

4.1 Which depletion chain files were used?

The depletion chain file is in the format of chain.xml file, which always starts with root element. The root element has one or more child elements, which contain nuclide name and can have additional information about decay modes, reactions, or fission product yields for a given nuclide. Information can be given about nuclide half-life in seconds, number of decay modes present, released decay energy in electron volts or the number of reactions present. [47]

Decay, reaction, and fission product data can be presented as a child element of element containing nuclide name. Which can describe accordingly type of the decay, daughter nuclide produced and branching ratio; present reactions type, energy released in electron volts and nuclide produced in the reaction and branching ratio; energy in electron volts at which yields are tabulated, fission products names, yields for each fission product. [47]

In this thesis we use three different depletion chain files. Depletion chain files for ENDF/B-VII.1 and ENDF/B-VIII.0 already exist, however a depletion chain file for JEFF-3.3 nuclear data library does not. For this reason, a new depletion chain file was created using code from github repository openmc-dev [41]. This code was modified to use the JEFF 3.3 library instead of ENDF/B-VII.1. Modified code can be seen in Appendix 1 [9.1].

To use JEFF-3.3, necessary files were collected from [40]. ENDF-6 files for neutron transport, radioactive data decay and neutron induced fission product yields were gathered to use for depletion chain assembly. Fission yields data was not in a desired format, therefore it had to be modified. Fission yields data separation code can be seen in Appendix 2 [9.2].

4.2 What model was used for depletion analyses?

An existing model created after Phase III-C benchmark was used. Phase III-C is an international burn-up calculation benchmark consisting of 35 calculation results covering different cross-section libraries from 16 institutes in 9 countries throughout Europe, Asia and USA. Phase III-C benchmark was created after the Fukushima Daiichi Nuclear Power Station accident in 2011, when the importance for criticality control of damaged fuel generated in 9x9 “STEP-3 BWR fuel” assemblies came to light. Last benchmark Phase III-B used 8x8 type fuel assembly, even though now 9x9 type fuel assemblies are more common, Phase III-C reflects this change and was constructed for 9x9 fuel assembly. [2]

In the model the geometry for a fuel assembly was constructed equivalent to the one in Phase III-B benchmark. An infinite two-dimensional array of BWR 9x9 type fuel assemblies, which are infinitely long, meaning having reflecting boundaries in at all sides, was set up by the defined geometry [2]. The geometry was set up by defining many different regions. All defined regions are depicted in Figure 8 with different colours.

The middle of the fuel assembly has a water channel (Figure 7), which had to be constructed of 9 different regions in the geometry (Figure 8). All fuel pins were constructed of circular regions, most

were constructed of a circular fuel region and a circle representing the rod around the fuel (Figure 8). However, some fuel rods are constructed of many different circles (Figure 8). The outmost circle still portrays the fuel cladding, but different circles in the middle represent either nuclear fuel or gadolinium oxide (Gd_2O_3) (Figure 8). The square around every fuel rod depicts water, it differs from the cooling water in the channel, because it has a different void fraction (Figure 8). Meaning around the fuel pins there is more evaporated water (Figure 7). The outermost square that surrounds the channel box is 0.67 cm thick cooling water, which is the same colour as the water channel in the middle (Figure 7). Cooling water has a 0% void fraction and the water around fuel bins can have a void fraction of 0%, 40% or 70%. Fuel pin cladding, water channel container and channel box are made of Zircalloy-2, which is an alloy consisting of Sn, Fe, Cr, Ni and Zr.

Different colours of fuel pins indicate the change of ^{235}U concentration throughout the fuel assembly. Yellow fuel pins correspond to 4.9wt% of ^{235}U in UO_2 , purple fuel pins correspond to 4.4wt% of ^{235}U in UO_2 , dark green fuel pins correspond to 3.4 wt% of ^{235}U in UO_2 , light green fuel pins correspond to 3.4wt% of ^{235}U in UO_2 , pink fuel pins correspond to 2,1wt% of ^{235}U in UO_2 and red fuel pins correspond to 3.4wt% of ^{235}U and 5.0wt% of Gd_2O_3 in $UO_2 - Gd_2O_3$ (Figure 7). Nuclear fuel assembly composition matches STEP-3 fuel assembly, which was also the type of fuel used in Fukushima Daiichi Nuclear Power Station [2]. The materials for geometry were all defined as OpenMC materials [48]. After defining the material all nuclei needed in this material were added one-by-one with atom percent. For example, for UO_2 with enrichment 4.9 wt% defining code can be seen in Appendix 3 [9.3].

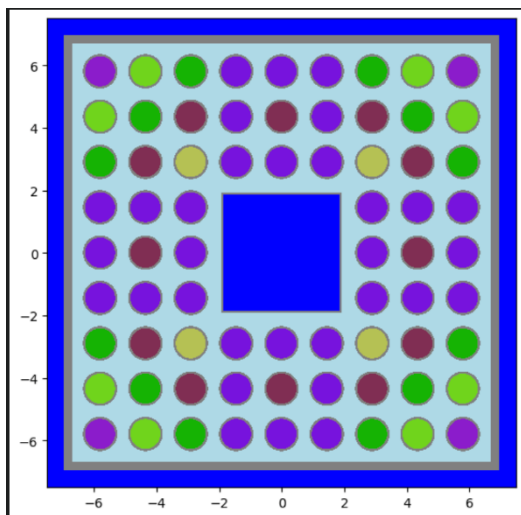


Figure 7: Fuel assembly model

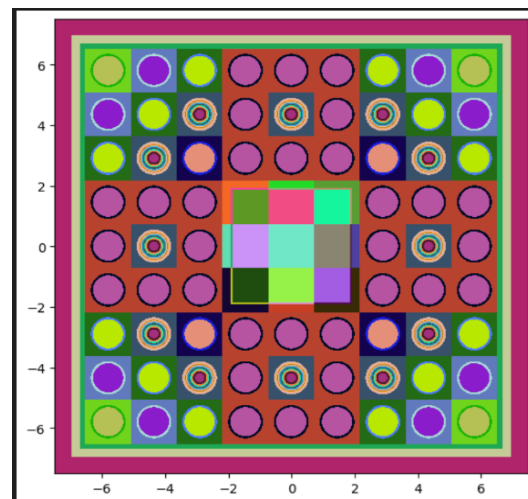


Figure 8: Geometry structure

5 Results on volatile gases inventory

Volatile gases generation in the model was converted to volatile gases generation in a BWR reactor by using the initial uranium inventory in a boiling water reactor with STEP 3 fuel assembly (170.9 kg) [49] and the initial uranium inventory in the model (~0.46 kg). As the model was 2D representation of a 3D object the calculations gave a smaller quantity of nuclide. To acquire a representation of 3D BWR fuel assembly the inventory of volatile gases had to be converted with a ratio. The ratio between BWR 3D fuel assembly and 2D model results was approximately 371 times. After the conversion, the results were also reworked to represent radioactivity using formulas [2],[3] and [4].

For further analysis, the results were also converted to represent volatile gasses production in BWRX-300 type of boiling water reactor. In BWRX-300 the initial uranium inventory is 44760 kilograms, and the reactor has 240 assemblies [21]. Meaning the initial uranium inventory in assembly is 186.5 kg. The ratio between real and model results was approximately 405 times. For more accurate results of BWRX-300 type of reactor the fuel assembly geometry in the model should be reworked to accurately represent BWRX-300 reactor fuel assembly.

5.1 Model validation and initial analyses

After setting up the geometry, calculations using three nuclear data libraries JEFF-3.3 and two versions of ENDF/B, an ENDF/B-VIII.0 and ENDF/B-VII.1 with three void fractions 0%, 40% or 70% were performed exactly like in the benchmark. A constant specific power of 25.3 MW/tHM was assumed for a final burn-up value of 50 GWd/tHM, the burn-up is considered as the mean over all fuel assemblies. Two cases of cooling times were considered after the burn-up: 0 and 5 years. The depletion process was simulated by using OpenMC depletion function [50]. Calculation results were summarised into nine H5 files.

First, the data about the quantity of each actinide and fission product used in Phase III-C benchmark was extracted, one code example in Appendix 4 [9.4]. Actinides and fission products discussed in benchmark can be seen in Appendix 5 [9.5] and Appendix 6 [9.6]. The data was then compared to the average results (Appendix 5,6 [9.5, 9.6]) gathered by countries participating in production of Phase III-C benchmark. This step was important to validate the model setup. For validating the data from last point calculated, spent nuclear fuel with burn-up of 50 GWd/tHM, that has had a cooling period of 5 years, was used (Appendix 4 [9.4]). For validation, every nuclei volume was received from openMC class function [51, 52] The function outputs the volume as one unit of volume per cubic centimetre of space ($1/\text{cm}^3$), which had to be multiplied by 10^{24} to match quantity unit in Phase III-C benchmark ($10^{24}/\text{cm}^3$). A graph to compare the calculated and expected values from Phase III-C benchmark is shown in Figure 9 and Figure 10.

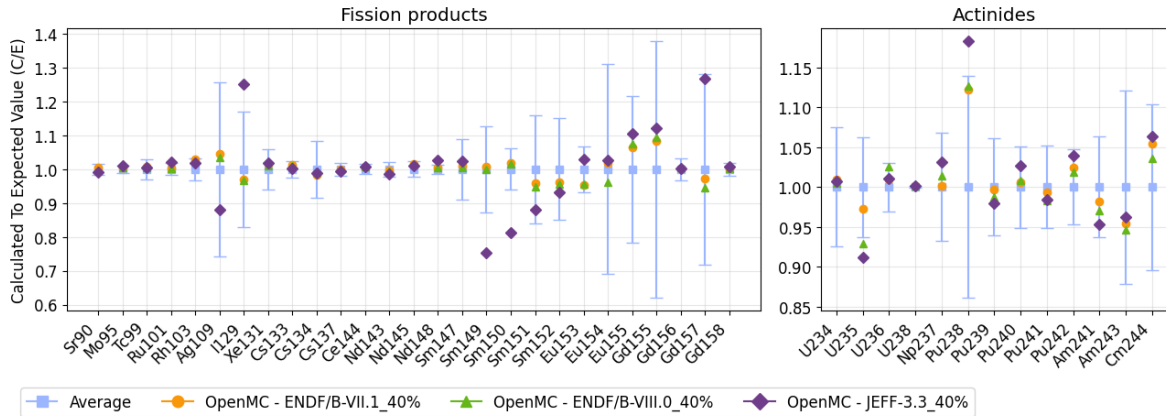


Figure 9: Validation using the void fraction of 40%

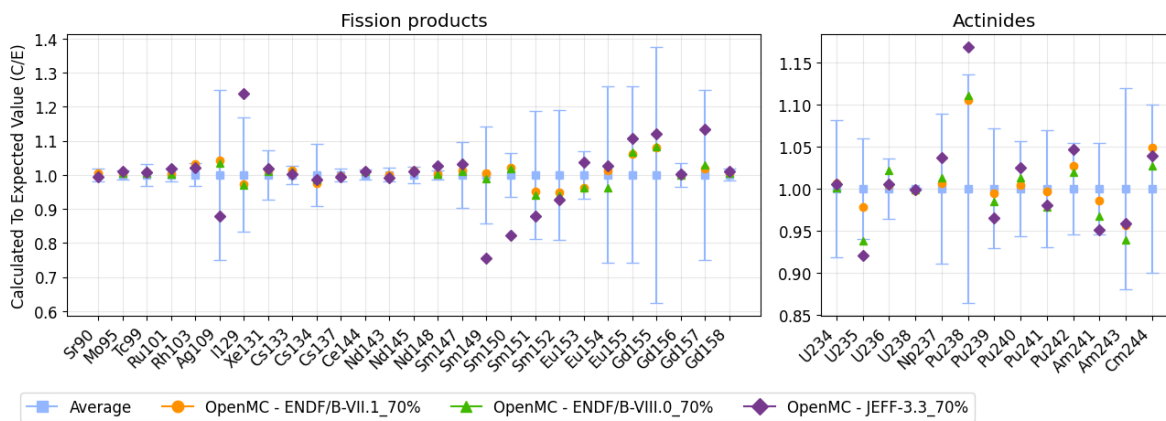


Figure 10: Validation using void fraction of 70%

Validation graphs (Figure 9, Figure 10) show that the results do not differ too much from average results gotten by the participating institutions. Nuclear data libraries used in the production of Phase III-C benchmark were JENDL-4, JEFF-3.1 and ENDF/B-VII.1 [2]. The graphs (Figure 9, Figure 10) illustrate that in many cases ENDF/B-VII.1 has the best overlap with the average results in the benchmark. That observation can be expected as ENDF/B-VII.1 was the only nuclear data library used in both this work and in the original calculations for Phase III-C benchmark.

After validating the model setup, mass data for volatile gases (^{129}I , ^3H , ^{85}Kr and ^{14}C) was extracted from the result files. From OpenMC class [51] a method for getting mass was used [52], as the method was quite new at the time of usage, it had a bug in the unit conversion. On that account the data was extracted in the original unit's grams and converted to kilograms, code example can be seen in Appendix 7 [9.7].

First, a comparison graph on void fraction 40% for different nuclear data libraries was constructed. Figure 11 shows JEFF-3.3 overestimating the production of ^{129}I , so in subsequent analysis for I129 the mass data will come from nuclear data library ENDF/B-VIII.0, as it is newer than ENDF/B-VII.1. ENDF/B-VIII.0 and ENDF/B-VII.1 underestimate the production of ^{14}C and ^3H , JEFF-3.3 will be used for further explorations with these nuclei. ENDF/B-VIII.0 overestimates the production of ^{129}Kr , ENDF/B-VII.1 will be used for further analyses.

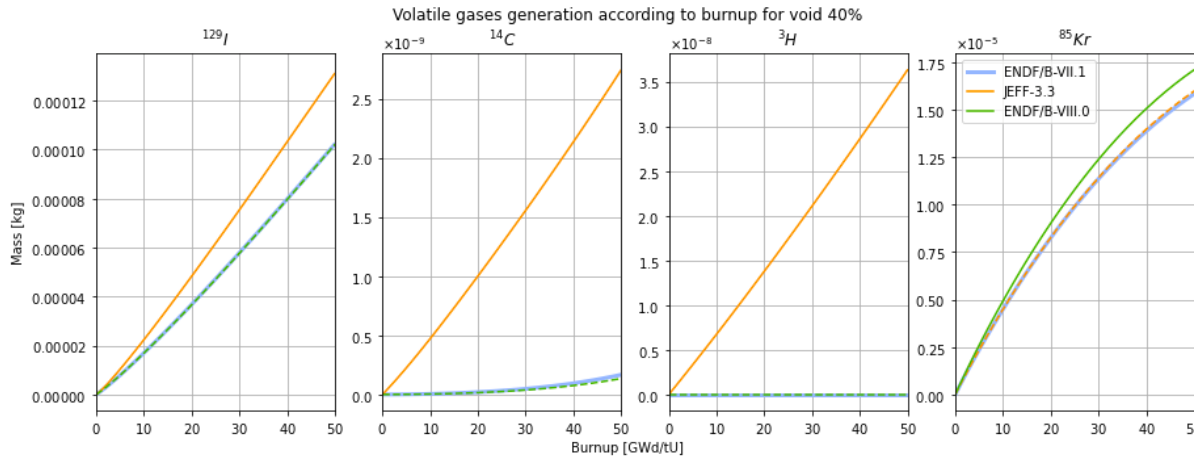


Figure 11: Graph comparing volatile gases production according to nuclear data libraries ENDF/B-VII.1, ENDF/B-VIII.0 and JEFF-3.3

5.2 ¹²⁹I production according to burn-up and void fraction

To analyse ¹²⁹I production as a function of burn-up and void fraction ENDF/B-VIII.0 nuclear data library was used. With all tested void fractions by the end of nuclear fuel life cycle in a STEP 3 type of fuel assembly the production of iodine-129 is between 0.036 and 0.038 kg, which is equal to radioactivity of $2.1 \cdot 10^5$ to $2.3 \cdot 10^5$ Bq (Figure 12). Compared to STEP 3, BWRX-300 fuel assembly produces a bit more iodine-129 (Figure 12). By the end of nuclear fuel life cycle around 50 GWd/tU with void fraction 70% produces the most around 0.043 kg or $2.5 \cdot 10^5$ Bq of iodine-129 (Figure 12).

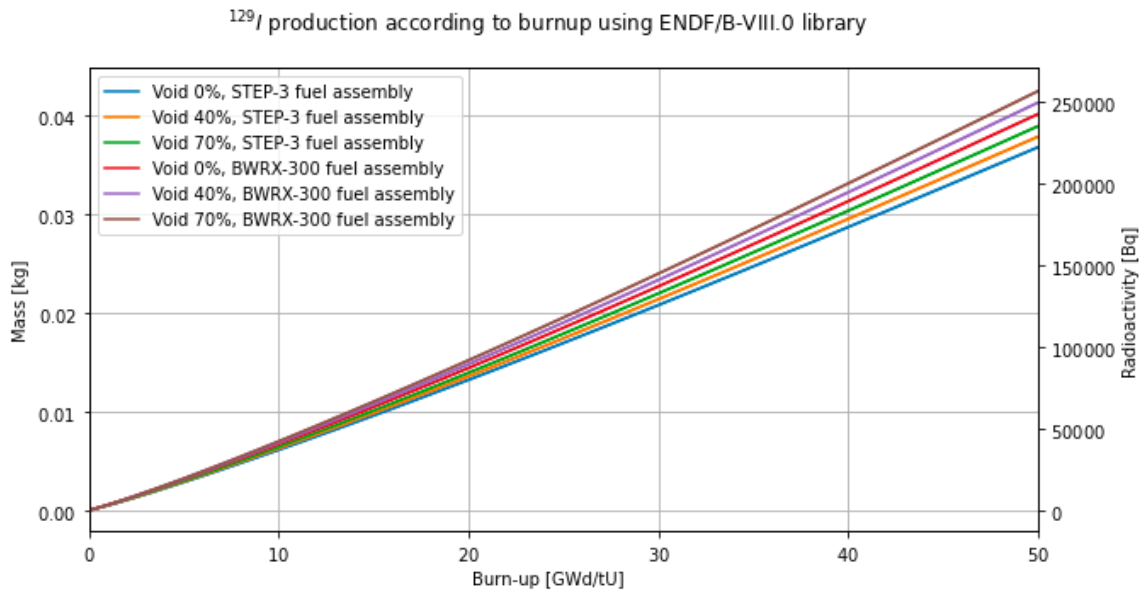


Figure 12: Iodine-129 production according to burn-up using different void fractions for STEP-3 and BWRX-300 fuel assembly

Figure 12 graph seems to have nearly constant gradient, which would indicate a close to linear relation between fuel assembly burn-up and produced ¹²⁹I nuclides total mass, volume and radioactivity in the assembly. Figure 13 shows a linear function fitted to the data. Figure 13. Iodine-129 production in STEP-3 and BWRX-300 fuel assembly fitted to linear and cubic functions, which indicated 2-degree polynomial to be a bit more accurate fit than first degree one. Both linear and

quadratic functions are acceptable alternatives for indicating I-129 production in fuel assembly during BWR operation as coefficient of determination (r^2) is about 0.9977 for linear function and 0.9999 for quadratic function, meaning functions describe accordingly 99.77% and 99.99% of our data variation.

1-degree polynomial underestimates and 2-degree polynomial overestimates with higher burn-up (Figure 13). Iodine-129 production increases during BWR operation until 50 GWd/tU according to fitted linear function by gradient of 4533 and BWRX-300 fuel assembly by gradient of 4942 (Figure 13). STEP-3 fuel assemblies production of Carbon-14 nuclide is described with linear function: $4533x - 5792$, and with quadratic function: $15.95x^2 + 3851x - 1631$ (Figure 13). BWRX-300 fuel assemblies production of Carbon-14 nuclide can be described with a linear function: $4947x - 6321$, and with a quadratic function: $17.4x^2 + 4203x - 1780$ (Figure 13).

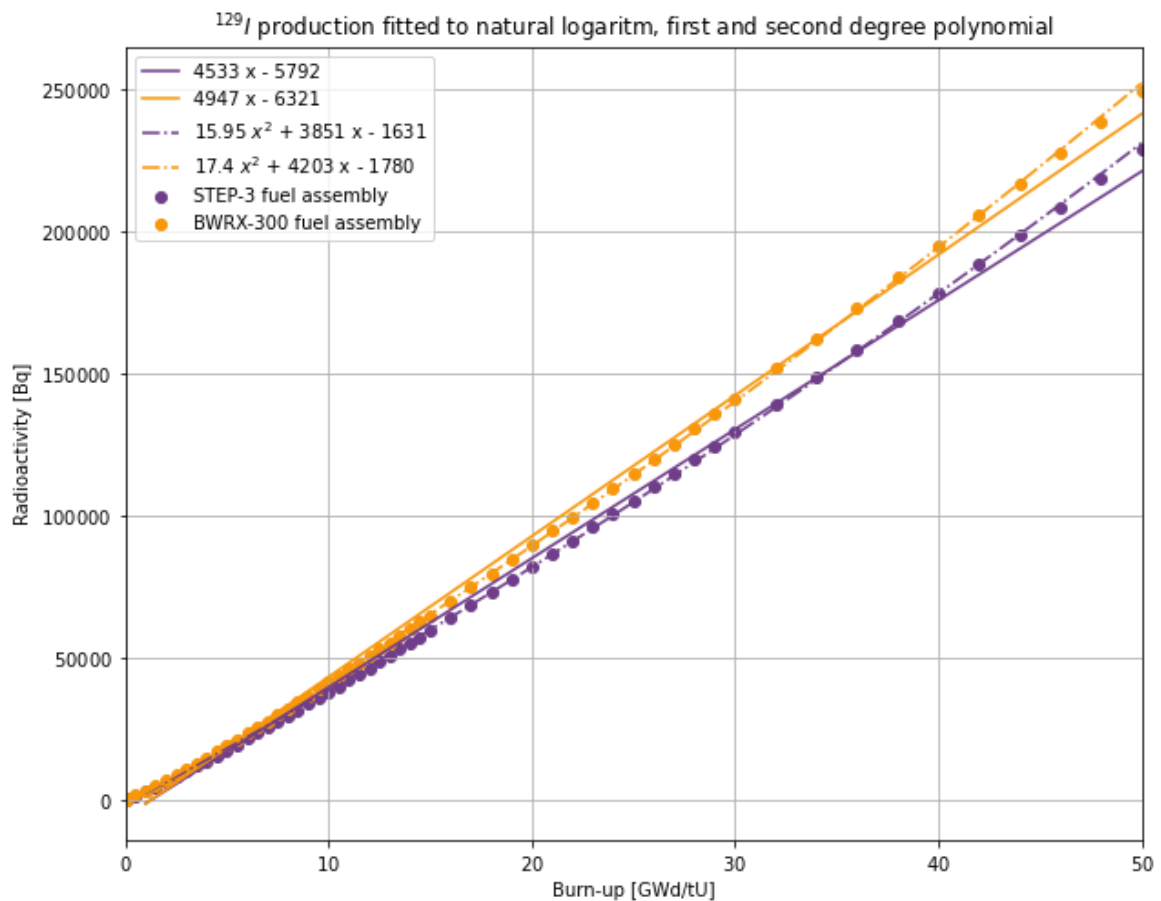


Figure 13. Iodine-129 production in STEP-3 and BWRX-300 fuel assembly fitted to linear and cubic function

In many research papers, Iodine-129 production is compared to Iodine-131 or even predicted from Iodine-131 concentration. As Iodine-131 has a shorter half-life of 8 days [53] it's concentration in biosphere is easier to measure on site. Figure 14 shows comparison of ^{131}I and ^{129}I production in a STEP-3 fuel assembly. ^{131}I graph behaviour is completely different from ^{129}I . After initial production spike ^{131}I concentration in the fuel assembly almost plateaus. This phenomenon can be explained by the half-life difference between the two iodine isotopes. With 8-day half-life ^{131}I starts to decay after the initial production. The decaying and production balance one another creating almost constant concentration of ^{131}I inside a fuel assembly.

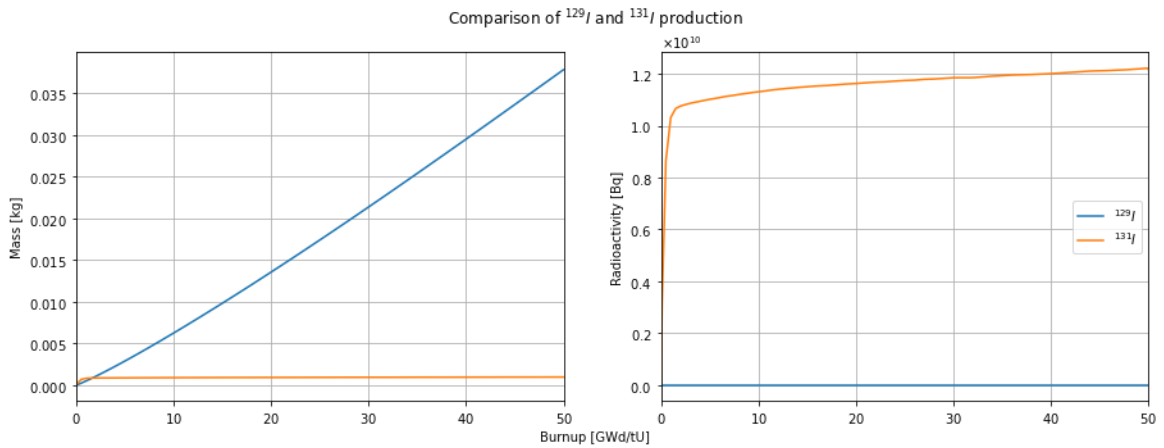


Figure 14: Comparison of iodine-129 and -131 production in a STEP-3 fuel assembly with void 40%

5.3 ^{14}C production according to burn-up and void fraction

To analyse ^{14}C production as a function of burn-up and void fraction JEFF-3.3 nuclear data library was used. With all tested void fractions by the end of nuclear fuel life cycle the production in a STEP 3 type of fuel assembly of Carbon-14 is around $1 \cdot 10^{-6}$ kg, which is equal to radioactivity of $1.6 \cdot 10^5$ Bq (Figure 15). Compared to STEP 3 BWRX-300 fuel assembly produces a bit more Carbon-14 (Figure 15). By the end of nuclear fuel life cycle around 50 GWd/tU with void fraction 70% produces the most around $1.6 \cdot 10^{-6}$ kg or $2.6 \cdot 10^5$ Bq of Carbon-14 (Figure 15).

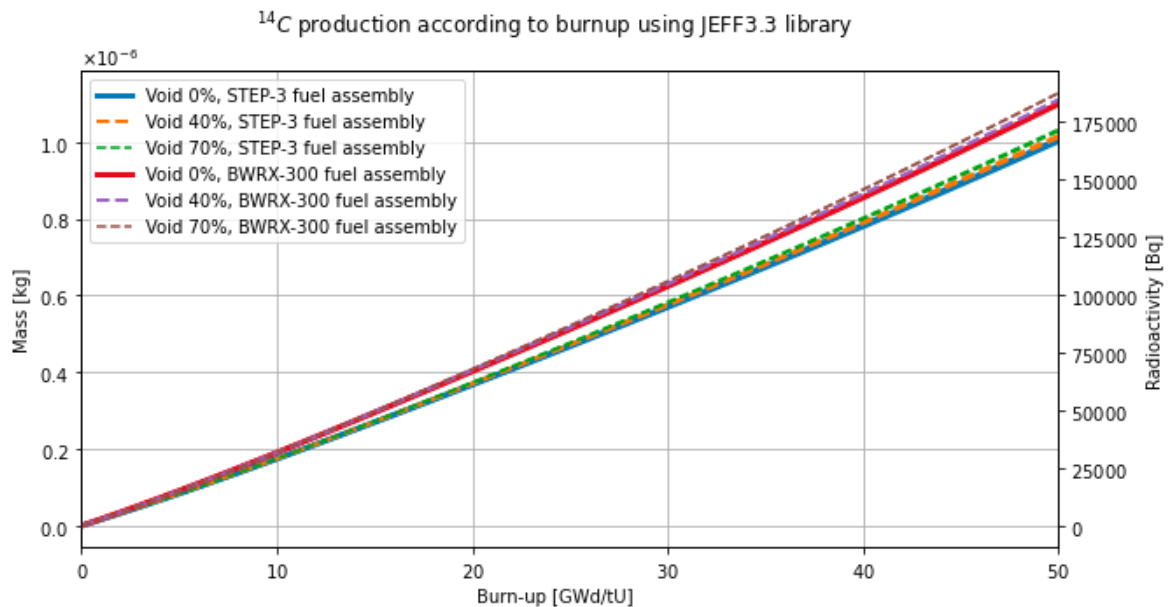


Figure 15: Carbon-14 production according to burn-up using different void fractions for STEP-3 and BWRX-300 fuel assembly

Figure 15 graph seems to have nearly constant gradient, which would indicate a close to linear relation between fuel assembly burn-up and produced ^{14}C nuclides total mass, volume and radioactivity in the assembly. Figure 16 shows a linear function fitted to the data. However, Figure 16 also indicates 2-degree polynomial to be a bit more accurate fit than first degree one. Both linear

and quadratic functions are acceptable alternatives for indicating C-14 production in fuel assembly during BWR operation as coefficient of determination (r^2) is about 0.9985 for linear function and 0.9999 for quartic function, meaning functions describe accordingly 99.85% and 99.99% of our data variation.

1-degree polynomial underestimates and 2-degree polynomial overestimates with higher burn-up (Figure 16). Carbon-14 production increases during BWR operation until 50 GWd/tU according to fitted linear function by gradient of 3311 and BWRX-300 fuel assembly by gradient of 3632 (Figure 16). STEP-3 fuel assemblies production of Carbon-14 nuclide is described with linear function: $3311x - 3212$, and with quadratic function: $9.7x^2 + 2896x - 681$ (Figure 16). BWRX-300 fuel assemblies production of Carbon-14 nuclide can be described with a linear function: $3632x - 3523$, and with a quadratic function: $10.64x^2 + 3177x - 747.1$ (Figure 16).

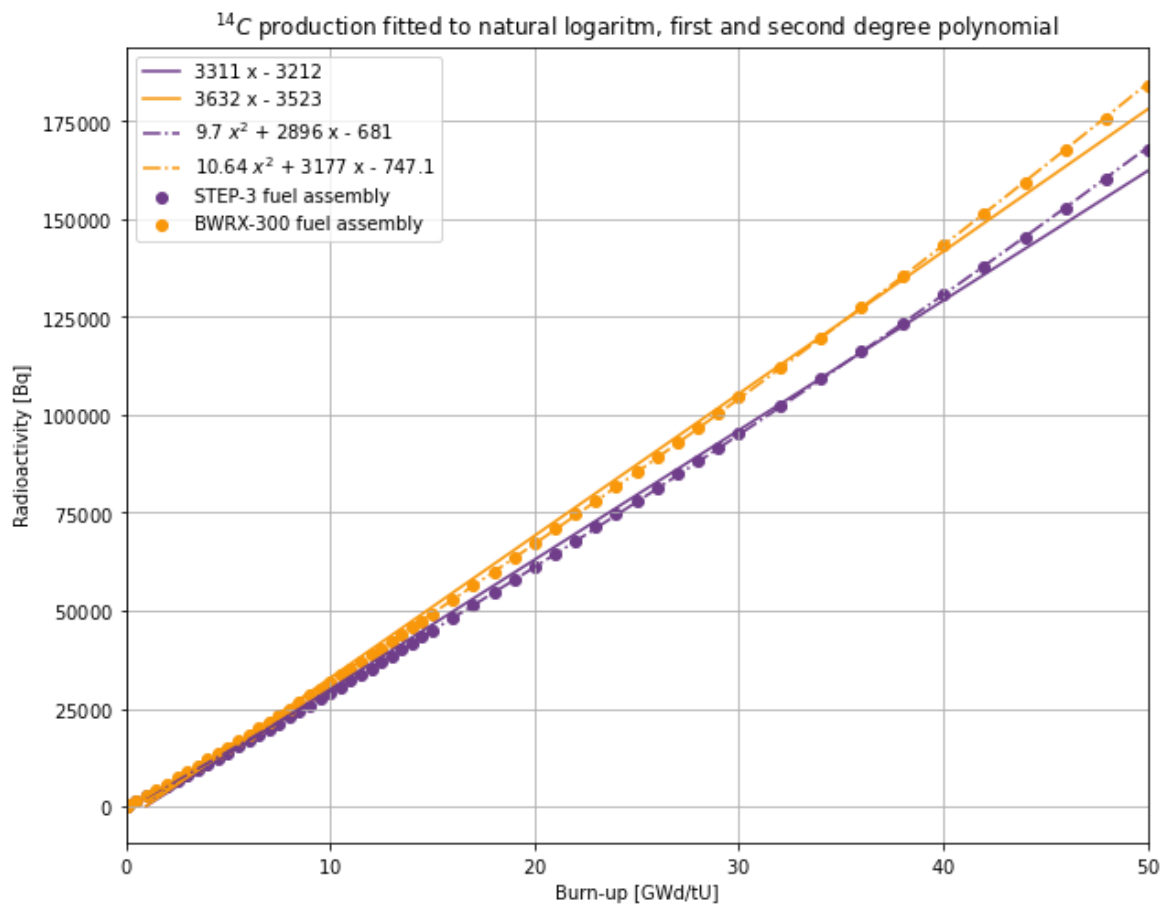


Figure 16: Carbon-14 production in STEP-3 and BWRX-300 fuel assembly fitted to linear and cubic function

5.4 ^3H production according to burn-up and void fraction

To analyse ^3H production as a function of burn-up and void fraction JEFF-3.3 nuclear data library was used. With all tested void fractions by the end of nuclear fuel life cycle the production of tritium in a STEP 3 type of fuel assembly is around $1.35 \cdot 10^{-5}$ kg, which is equal to radioactivity of 4.9 GBq

(Figure 17). For tritium void fraction does not play a role in the amount produced. The difference between the mass of hydrodgen-3 with varying void fractions is only minuscule and that probably comes from the randomness on Monte Carlo method. Compared to STEP 3 BWRX-300 fuel assembly produces a bit more tritium (Figure 17). By the end of nuclear fuel life cycle around 50 GWd/tU with void fraction 70% produces the most around $1.45 \cdot 10^{-5}$ kg or 5.2 GBq of tritium (Figure 17).

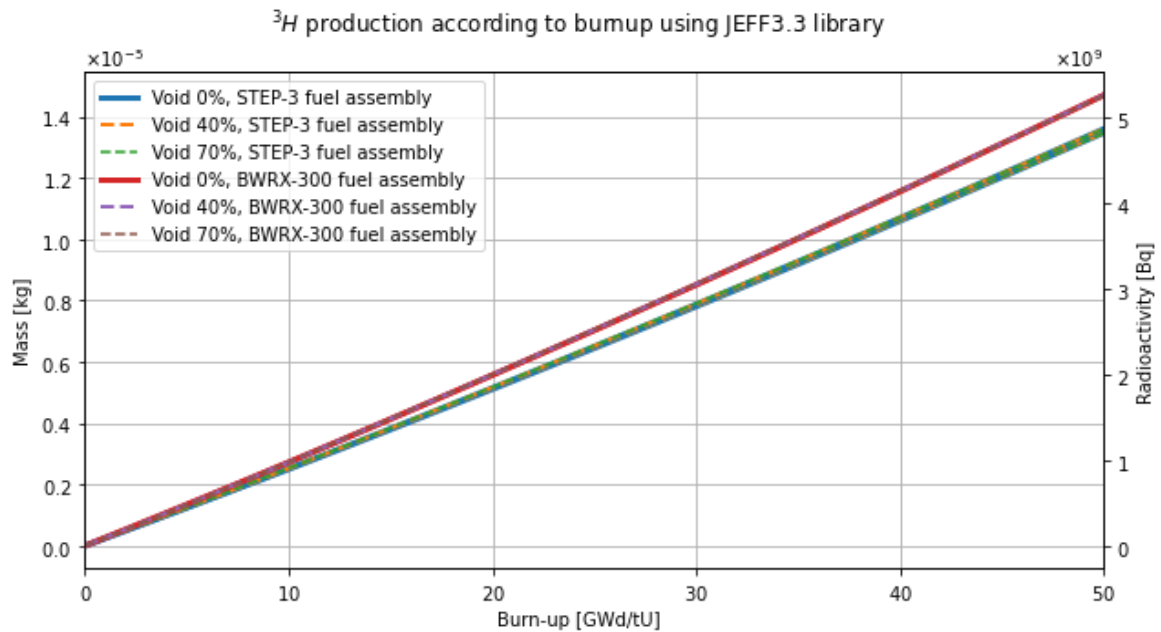


Figure 17: Tritium production according to burn-up using different void fractions for STEP-3 and BWRX-300 fuel assembly

Figure 17 graph seems to have nearly constant gradient, which would indicate a close to linear relation between fuel assembly burn-up and produced ^3H nuclides total mass, volume and radioactivity in the assembly. Figure 18 shows a linear function fitted to the data. However, Figure 18 also indicates 2-degree polynomial to be a bit more accurate fit than first degree one. Both linear and quadratic functions are acceptable alternatives for indicating H-3 production in fuel assembly during BWR operation as coefficient of determination (r^2) is about 0.9994 for linear function and 0.9999 for quartic function, meaning functions describe accordingly 99.94% and 99.99% of our data variation.

1-degree polynomial underestimates and 2-degree polynomial overestimates with higher burn-up (Figure 18). Tritium production increases during BWR operation until 50 GWd/tU according to fitted linear function by gradient of 0.096 and BWRX-300 fuel assembly by gradient of 0.10 (Figure 18). STEP-3 fuel assemblies production of Tritium nuclide is described with linear function: $9.64 \cdot 10^7 x - 4.58 \cdot 10^7$, and with quadratic function: $1.65 \cdot 10^5 x^2 + 8.94 \cdot 10^7 x - 2.81 \cdot 10^6$ (Figure 16). BWRX-300 fuel assemblies production of Carbon-14 nuclide can be described with linear function: $1.04 \cdot 10^8 x - 4.95 \cdot 10^7$, and with quadratic function: $1.78 \cdot 10^5 x^2 + 9.66 \cdot 10^7 x - 3.03 \cdot 10^6$ (Figure 16).

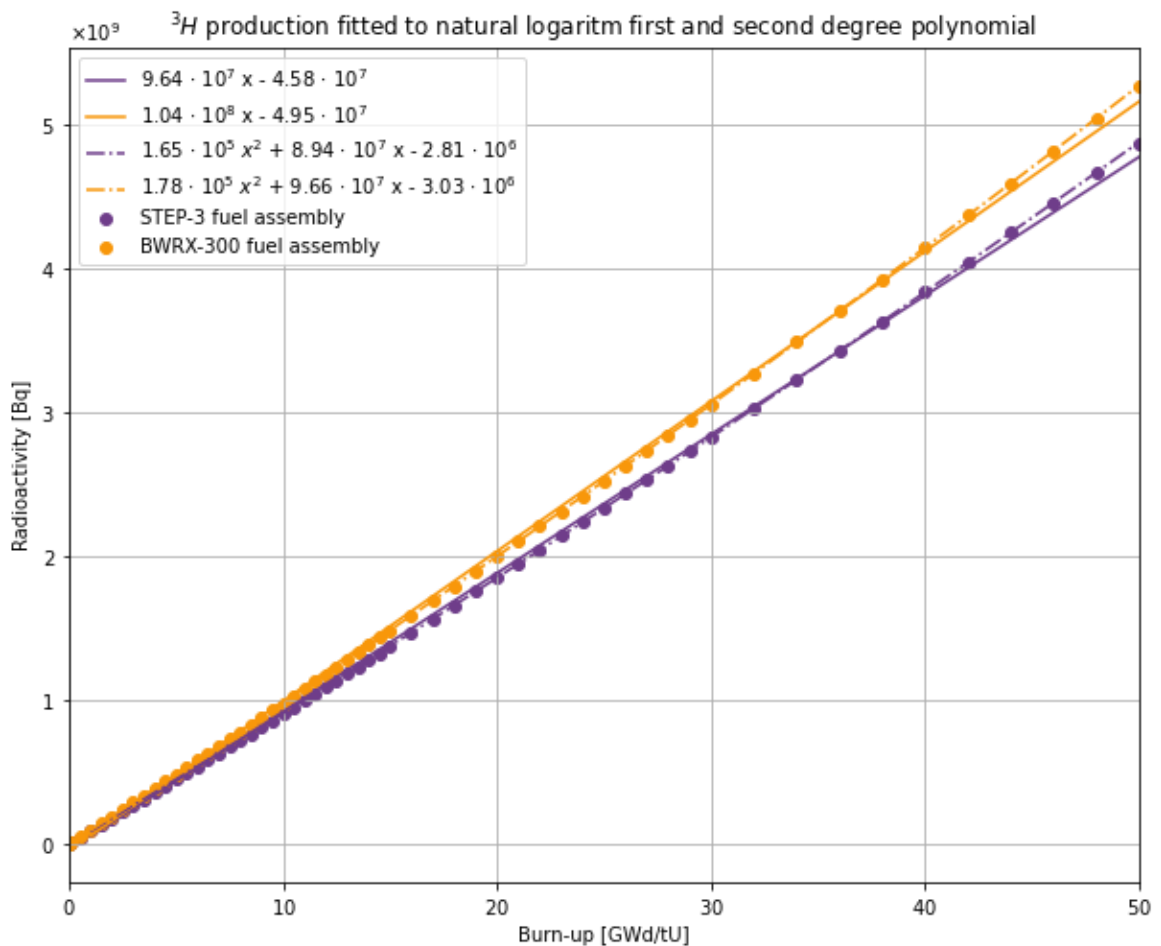


Figure 18: Tritium production in STEP-3 and BWRX-300 fuel assembly fitted to linear and cubic function

5.5 ${}^{85}\text{Kr}$ production according to burn-up and void fraction

To analyse ${}^{85}\text{Kr}$ production as a function of burn-up and void fraction ENDF/B-VII.1 nuclear data library was used. With all tested void fractions by the end of nuclear fuel life cycle in a STEP 3 type of fuel assembly the production of krypton-85 is between 0.0056 and 0.006 kg, which is equal to radioactivity of 81 to 87 GBq (Figure 19). Compared to STEP 3 BWRX-300 fuel assembly produces a bit more krypton-85 (Figure 19). By the end of nuclear fuel life cycle around 50 GWd/tU with void fraction 70% produces the most around 0.0066 kg or 95 GBq of krypton-85 (Figure 19).

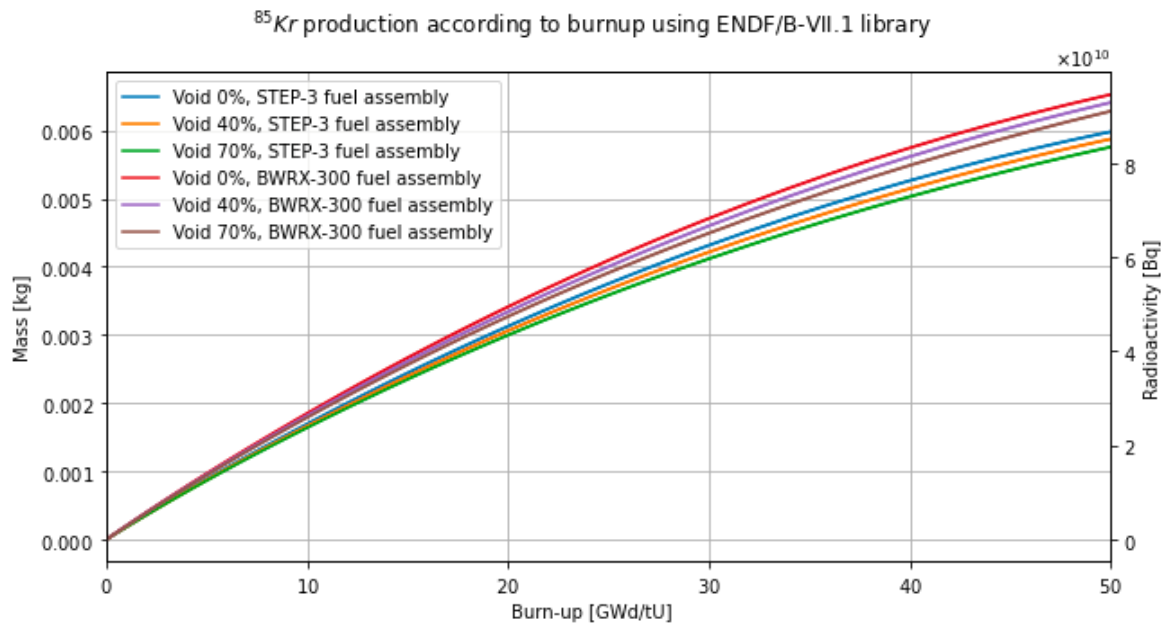


Figure 19: Krypton-85 production according to burn-up using different void fractions for STEP-3 and BWRX-300 fuel assembly

Figure 19 graph seems to have nearly constant gradient, which would indicate a close to linear relation between fuel assembly burn-up and produced ⁸⁵Kr nuclides total mass, volume and radioactivity in the assembly. Figure 20 shows a linear function fitted to the data. However, Figure 20 also indicates 2-degree polynomial to be a more accurate fit than first degree one. Linear function is suitable for indicating Kr-85 production with lower burn-up, yet with higher burn-up it tends to overestimate the total volume of producer Krypton-85 nuclide (Figure 20). On account of that, quadratic functions is a preferable alternative for accurately indicating ⁸⁵Kr production in fuel assembly during BWR operation. This is also confirmed by coefficient of determination (r^2) which for linear function is 0.9842 and for quadratic function is 0.9999, meaning the functions describe accordingly 98.42% and 99.99% of our data variation.

Krypton-85 production increases during BWR operation until 50 GWd/tU according to fitted linear function by gradient of $1.81 \cdot 10^9$ and BWRX-300 fuel assembly by gradient of $1.98 \cdot 10^9$ (Figure 20). STEP-3 fuel assemblies production of Krypton-85 nuclide is described with a linear function: $1.81 \cdot 10^9 x + 4.78 \cdot 10^9$, and with a quadratic function: $-1.73 \cdot 10^7 \cdot x^2 + 2.55 \cdot 10^9 \cdot x + 2.67 \cdot 10^8$ (Figure 20). BWRX-300 fuel assemblies production of Carbon-14 nuclide can be described with a linear function: $1.98 \cdot 10^9 x + 4.78 \cdot 10^9$, and with a quadratic function: $-1.89 \cdot 10^7 \cdot x^2 + 2.79 \cdot 10^9 \cdot x + 2.91 \cdot 10^8$ (Figure 20).

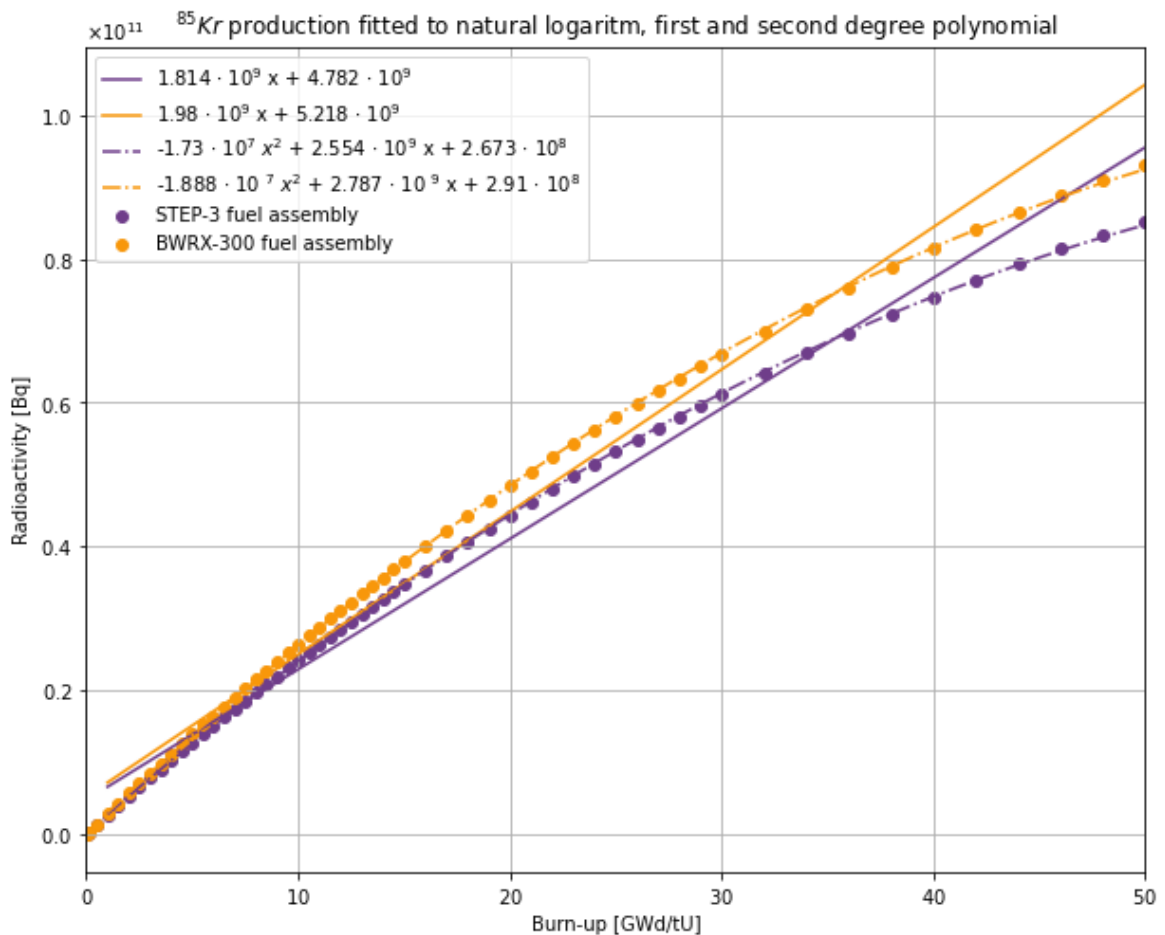


Figure 20: Krypton-85 production in STEP-3 and BWRX-300 fuel assembly fitted to linear and cubic function

5.6 Volatile gases

Looking at various isotope production as a function of burn-up and void fraction is important because Fukushima Daiichi Nuclear Power Station has shown that during decommissioning criticality control of damaged nuclear fuel becomes an issue. To assess criticality parameters of damaged fuel the inventory of nuclide in average spent nuclear fuel as a function of burn-up is a required input.

Isotope production as a function of burn-up is also interesting as it illustrates nicely the phenomena of fresh nuclear fuel gaining radioactivity during the NPP operation. Furthermore, through similar graphs the compositional changes in nuclear fuel throughout NPP operational years and cooling period (spent nuclear fuel storage period) can be monitored and studied. Looking at various isotope production as a function of void fraction is captivating as it shows isotopes concentration in different parts of the reactor core, while demonstrating the fact that while boiling biggest gas concentration and production is at the top of reactor fuel assembly, where the void fraction is the highest.

The research of this thesis shows GE boiling water reactors (Fukushima type of reactors) generating fewer volatile gases per fuel assembly than BWRX-300, as the nuclear fuel has a bit less initial

uranium in it. However volatile gasses production is largely dependent on a NPP size, and how long the fuel is kept inside the reactor(burn-up). GE Hitachi Nuclear Energy's (GEH's) BWRX-300 is designed as a 300 MW Small Modular Reactor (SMR), which makes it smaller than all units in Fukushima Daiichi reactors. This in turn also makes the overall volatile gases production per year in a BWRX-300 less than in Fukushima Daiichi reactors.

Results also show void fraction being typically a factor in a volatile gas production. In most cases bigger void fraction produces more volatile gases. Meaning in nuclear reactor volatile gases are more concentrated in the upper part of the reactor, where there is more evaporated water and therefore the void fraction is also higher. The only volatile fission product considered in this thesis that is not dependant on void fraction is tritium. This phenomenon could be caused by the fact that the calculations with different void fractions use the same burn-up. Meaning this model's base assumption is that with all void fractions the same amount of energy is extracted from nuclear fuel. This implies more neutrons and/or different base conditions, as neutrons would have to have more energy. These factors can cause more fission products with a bigger void factor.

Production variation for three volatile gases can be described by a linear function with approximately 99% accuracy. ^{85}Kr and ^{131}I are the outlier in this case. ^{131}I has a short half-life and starts to decay during fuel lifetime, which causes the gas production to plateau. ^{85}Kr has the shortest half-life (10,73 years) out of 4 long-lived volatile gases in this thesis. In Fukushima Daiichi Nuclear Power Station Unit 1 nuclear fuel would achieve burn-up 50 GWd/tU after approximately 13 years, meaning ^{85}Kr also starts to decay during reactor operation, which in turn make the production of nuclide vary from 1-degree polynomial more with higher burn-up. Better representation for ^{85}Kr nuclide production is a 2-degree polynomial.

All four long-lived volatile gases are described better by quadratic function, as for ^{85}Kr it references the decaying better and for ^{129}I , ^3H and ^{14}C considers the production of other nuclide which can either during decay or fission processes create these volatile gases. The relation between BWR fuel burn-up and volatile gas inventory is positive, when one variable is increased the other also increases. This phenomenon can be explained by fuel depleting and producing more by-products.

5.7 Discussion and conclusions

The main objective of this thesis, estimating the evolution of four long-lived volatile gases ^{129}I , ^{14}C , ^3H , ^{85}Kr inventory over fuel lifetime in a BWR using OpenMC capabilities, has been fulfilled. The source term created from study results can be seen in Appendix 8. Source term STEP-3 fuel assembly [9.8]. For this purpose, depletion analyses on BWR fuel assembly were constructed with OpenMC, which uses Monte Carlo method as a basis to calculate each particle's path. This analysis gave an overview of nuclide production in nuclear fuel throughout BWR operation.

The comparison of SMR BWRX-300 and STEP-3 fuel assemblies shows the latter generating fewer volatile gases. However overall volatile gases production per year in a BWRX-300 is less than in Fukushima Daiichi reactors, due to the reactor size and fuel burn-up. BWRX-300 results were

converted from STEP-3 fuel assembly. For a more accurate comparison, BWRX-300 volatile gasses inventory could be reworked using the same technique with the geometry of the fuel assembly changed to a 10X10 fuel assembly with two water channels.

Void fraction difference in reactors could also be a contributor to volatile gases inventory variation. In the case of 3 volatile gases (^{129}I , ^{14}C , ^{85}Kr) researched in this thesis, bigger void fraction meant higher total mass of this nuclide. Tritium production did not show signs of being dependant on void fraction. Next to the positive relation between void fraction and volatile gases generation BWR fuel burn-up and volatile gas inventory also has a positive relation. Higher burn-up also meant a higher total mass of volatile gas.

Long-lived volatile gases production can be described as a linear function. Considering four volatile gases analysed in this thesis 1-degree polynomial accurately presented 98% of the variation in the production of volatile gases. However, 2-degree polynomial was a better representation, as it could also take into account ^{85}Kr decaying process and ^{129}I , ^3H , ^{14}C being produced from other fission products in either fission or decaying processes.

By the fuel lifetime end (burn-up 50 GWd/tU) ^{129}I nuclides have the biggest total mass concentration out of long-lived volatile gases considered in this thesis. Highest radioactivity is emitted by ^{85}Kr isotopes at burn-up 50 GWd/tU. ^{85}Kr has the shortest half-life of all long-lived volatile isotopes considered in this thesis. ^{129}I has a significantly longer half-life than ^{85}Kr , which in turn makes ^{129}I radioactivity considerably smaller, even though the total mass in BWR fuel assembly is bigger.

5.8 Further research

For future research, it is recommended to expand the computational framework from a 2D to a 3D model for the depletion analyses to improve the realism of the simulations to better mirror real-world conditions and/or to evaluate the potential error coming from 2D versus 3D approach. By transitioning from a two-dimensional representation to a three-dimensional one, a broader spectrum of factors could be described and simulated to make for a more realistic inventory of volatile gases. Furthermore, for better representativeness of the BWRX-300 volatile gasses inventory the same technique could be used with the geometry of the fuel assembly changed to a 10X10 fuel assembly with two water channels. This change in the geometry would indicate a more accurate representation BWRX-300 fuel assembly volatile gases inventory.

6 Abstract

In this thesis the evolution of four long-lived volatile gases ^{129}I , ^{14}C , ^3H , ^{85}Kr inventory over fuel lifetime in a BWR was estimated. For this purpose, depletion analyses on BWR fuel assembly were constructed with OpenMC, which uses Monte Carlo method as a basis to calculate each particle's path. STEP-3 type of fuel assembly was used as a basis for this study, which was modelled after the OECD/NEA Phase III-C benchmark. For volatile gases representation three nuclear data libraries evaluated by a recognized evaluation group (JEFF-3.3, ENDF/B-VII.1, ENDF/B-VIII.0) were used. Depletion calculation results were verified against results gathered in Phase III-C benchmark from various nuclear data institutes in Asia, Europe and USA. The analysis gave an overview of nuclide production in nuclear fuel throughout BWR operation. The volatile gases production was presented as a function of burn-up and void fraction. The inventory was represented as a total mass of nuclides in kilograms and as a total radioactivity in becquerels.

Inventory analyses showed positive correlation between fuel burn-up and volatile gas generation. Higher fuel burn-up means more production of volatile isotopes. Positive relation was observed also between void fraction and volatile gas concentration in BWR fuel assembly for 3 out of 4 long-lived volatile gases: ^{129}I , ^{14}C and ^{85}Kr . Analysis on tritium did not show any link between void fraction and ^3H nuclides production. Polynomial functions were fitted to volatile gases production graphs to describe the correlation between burn-up and isotope production. Approximation graph analyses displayed linear function as an acceptable reference point to estimate volatile gas production. However, quadratic function was deemed as a better option, for considering additional variables (fission product fission and decay processes, volatile gas isotope decaying) to ^{235}U fission. Additionally, source term for volatile gases production in a STEP-3 fuel assembly was created (Appendix 8 [9.8]).

7 Annotatsioon

Käesolevas lõputöös hinnati nelja pikaajalise lenduva gaasi ^{129}I , ^{14}C , ^3H ja ^{85}Kr inventuuri keevaveereaktoris kütuse eluea jooksul. Selleks loodi keevaveereaktori kütusekoostel põhineva vaestumisanalüüs. Analüüsi läbiviimiseks kasutati OpenMC-d, mis kasutab Monte Carlo meetodit iga osakese trajektoori ennustamiseks. Uurimiseks kasutati baasina STEP-3 tüüpi kütusekoostet, mis mudeldati OECD/NEA *Phase III-C benchmark* võrdlusmudeli alusel. Lenduvate gaaside esindamiseks kasutati kolme tuumaandmete kogu: JEFF-3.3, ENDF/B-VII.1, ENDF/B-VIII.0. Kütusekoostise vaestumisarvutuse tulemusi kontrolliti vastu erinevate tuumaenergia instituutide tulemusi, mis on kajastatud *Phase III-C benchmark's*. Analüüs andis ülevaate nukliidide tootlusest tuumkütuse koostus kogu keevaveereaktori tööaja vältel. Lenduvate gaaside tootmine esitati funktsioonina sõltuvuses utiliseerimismäärast ja veeauruosakaalust. Nukliidide kogust kajastati kahel viisil: kogumassina kilogrammides ja koguradioaktiivsusega becquerelides.

Inventuuri analüüsid näitasid positiivset seost *utiliseerimismäär*a ja lenduvate gaaside tekkimise vahel. Kõrgem kütuse *utiliseerimismäär* tähendab suuremat lenduvate isotoopide tootlust. Keevaveereaktori kütusekoostus täheldati positiivset seost ka veeauruosakeelu ja lenduvate gaaside kontsentratsiooni vahel kolme pikaajalise lenduva gaasi puhul neljast: ^{129}I , ^{14}C ja ^{85}Kr . Triitiumi analüüs ei näidanud mingit seost veeauruosakaalu ja ^3H nukliidide tootluse vahel. Lenduvate gaaside isotoopide tootlusgraafikutele sobitati polünoomfunktsioone kirjeldamaks *utiliseerimismäär*a ja isotoopide produktsiooni vahelist seost. Töö tulemused näitavad, et lenduvate gaaside tootluse ligikaudseks hindamiseks on lineaarne funktsioon vastuvõetavaks lähtepunkt, kuid ruutfunktsioon on parem valik. Ruutfunktsioon kajastab ^{235}U lõhustumisele lisaks täiendavaid muutujaid: tuuma lõhustumisproduktide lõhustumis ja lagunemis protsesse, lenduvate gaaside isotoopide lagunemist. Lisaks loodi lenduvate gaaside tootluse lähteallikas STEP-3 kütusekoostu jaoks (Lisa 8 [9.8]).

Acknowledgements

I would like to express gratitude towards my supervisor Marti Jeltsov, PhD, Research Fellow KBFI, for proposing the topic of this thesis and supervising this thesis. Additionally, I would like to thank Hando Tohver, MSc, Junior Research Fellow UT, who helped me throughout the whole process of constructing this thesis.

8 References

- [1] P. Baron, E. Collins, S. Cornet, G. D. Angelis, B. DelCul, G. Grassi, V. Ignatiev, I.-T. Kim, J. Law, T. Matsumura, M. Miguiditchian, Y. Morita, R. Taylor, J. Turner and J. Uhler, "Treatment of Volatile Fission Products," Nuclear Energy Agency, 2022.
- [2] K. Suyam, Y. Uchida, T. Kashima, T. Ito and T. Miyaji, "Burn-up Credit Criticality Safety Benchmark," Nuclear Energy Agency, 2016.
- [3] P. K. Romano, N. E. Horelik, B. R. Herman, A. G. Nelson, B. Forget and K. Smith, "OpenMC: A state-of-the-art Monte Carlo code for research and development," *Annals of Nuclear Energy*, pp. 90-97, August 2015.
- [4] D. Brown, M. Chadwick, R. Capote, A. Kahler, A. Trkov, M. Herman, A. Sonzogni, Y. Danon, A. Carlson, M. Dunn, D. Smith, G. Hale, G. Arbanas, R. Arcilla, C. Bates, B. Becker, F. Brown, R. Casperson, J. Conlin and D. Cullen, "ENDF/B-VIII.0: The 8th Major Release of the Nuclear Reaction Data Library with CIELO-project Cross Sections, New Standards and Thermal Scattering Data," *Nuclear Data Sheets*, pp. 1-142, February 2018.
- [5] M. Chadwick, M. Herman, P. Obložinský, M. Dunn, Y. Danon, A. Kahler, D. Smith, B. Pritychenko, G. Arbanas, R. Arcilla, R. Brewer, D. Brown, R. Capote, A. Carlson, Y. Cho, H. Derrien, K. Guber, G. Hale, S. Hoblit, S. Holloway and T. Johnson, "ENDF/B-VII.1 Nuclear Data for Science and Technology: Cross Sections, Covariances, Fission Product Yields and Decay Data," *Nuclear Data Sheets*, vol. Volume 112, no. Issue 12, pp. 2887-2996, 2011.
- [6] Massachusetts Institute of Technology, UChicago Argonne LLC, and OpenMC contributors, "Official Data Libraries," 2011-2023. [Online]. Available: <https://openmc.org/official-data-libraries/>. [Accessed 6 May 2024].
- [7] B. Pershagen, *Light Water Reactor Safety*, Nyköping: pergamon Press, 1996.
- [8] K. Iskar, H. Ormus, A. Vragar, K. Kallemets, A. Paist, M. Jelotsev, K. Kööp, M. Pukari and A. Hektor, *Tuuma Energia, Postimees Kirjastus*, 2021.
- [9] United States Nuclear Regulatory Commission, "The Boiling Water Reactor(BWR)," United States Nuclear Regulatory Commission, 17 August 2017. [Online]. Available: <https://www.nrc.gov/reading-rm/basic-ref/students/animated-bwr.html>. [Accessed 5 March 2024].
- [10] K. Tucek, "Neutronic and Burnup Studies of Accelerator-driven Systems Dedicated to Nuclear Waste Transmutation," Royal Institute of Technology Department of Physics, Stockholm, 2004.
- [11] Nuclear Power, "Precursors of Delayed Neutrons," Nuclear Power, 2024. [Online]. Available: <https://www.nuclear-power.com/nuclear-power/fission/delayed-neutrons/precursors-of-delayed-neutrons/>. [Accessed 26 April 2024].
- [12] Nuclear Power, "Fuel Burnup," Nuclear Power, 2024. [Online]. Available: <https://www.nuclear-power.com/nuclear-power/reactor-physics/reactor-operation/fuel-burnup/>. [Accessed 28 February 2024].
- [13] Nuclear Power, "Composition of Spent Nuclear Fuel," Nuclear Power, 2024. [Online]. Available: <https://www.nuclear-power.com/nuclear-power-plant/nuclear-fuel/spent-fuel/composition-of-spent-nuclear-fuel/>. [Accessed 28 February 2024].
- [14] Office of Nuclear Energy, "5 Fast Facts about Spent Nuclear Fuel," U.S. Department of Energy, 3 October 2022. [Online]. Available: <https://www.energy.gov/ne/articles/5-fast-facts-about-spent-nuclear-fuel>. [Accessed 28 February 2024].

- [15] International Atomic Energy Agency, "Getting to the Core of the Nuclear Cycle From the mining of uranium," Department of Nuclear Energy, Vienna.
- [16] United States Nuclear Regulatory Commission, "What is Spent Nuclear Fuel?," United States Nuclear Regulatory Commission, 19 March 2020. [Online]. Available: <https://www.nrc.gov/reading-rm/basic-ref/students/science-101/what-is-an-spent-fuel.html>. [Accessed 28 February 2024].
- [17] Y. Nakano and T. Okubo, "Plutonium isotopic composition of high burnup spent fuel discharged from light water reactors," *Annals of Nuclear Energy*, pp. 2689-2697, December 2011.
- [18] C. Brown, K. Hartley and J. Hulsman, "Extended Power Uprates and 2-yr Cycles for BWRs - Where Do We Go from Here?," *Nuclear Technology*, p. 120–125, 2005.
- [19] V. P. Guinn, "Radioactivity," in *Encyclopedia of Physical Science and Technology (Third Edition)*, California, University of California, 2003, pp. 661-674.
- [20] World Nuclear Association, "Fukushima: Background on Reactors," World Nuclear Association, 2016-2023. [Online]. Available: <https://world-nuclear.org/information-library/safety-and-security/safety-of-plants/appendices/fukushima-reactor-background.aspx>. [Accessed 16 April 2024].
- [21] GE Hitachi Nuclear Energy, "BWRX-300 General Description," GE-Hitachi Nuclear Energy Americas LLC, 2023.
- [22] E. H. Uguru, M. F. B. A. Sapli, S. A. Sani, M. U. Khandaker, M. H. Rabir and J. A. K. D. Bradley, "Impact of weight percent gadolinium and the number of its fuel rods on the neutronic and safety parameters," *Radiation Physics and Chemistry*, November 2021.
- [23] H. M. Dalle, J. R. L. d. Mattos and M. S. Dias, "Enriched Gadolinium Burnable Poison for PWR Fuel – Monte Carlo Burnup Simulations of Reactivity," in *Current Research in Nuclear Reactor Technology in Brazil and Worldwide*, InTech, 2013.
- [24] P. M. Altomare, M. Barber, N. Lord and D. Nainan, "Assesment of Waste Managment of Volatile Radionuclides," The MITRE Corporation, Virginia, 1979.
- [25] P. Povinec, M. Gera, K. H. K. Holy, G. Lujaniene, M. Nakano, W. Plastino, I. Sykora, J. Bartok and M. Gazak, "Dispersion of Fukushima radionuclides in the global atmosphere and the ocean," *Applied Radiation and Isotopes*, pp. 383-392, November 2013.
- [26] ANDRA, "Evaluation de la faisabilité du stockage géologique en formation argileuse," Châtenay-Malabry, 2005.
- [27] A. L. Nichols, D. L. Aldama and M. Verpelli, "HANDBOOK OF NUCLEAR DATA FOR SAFEGUARDS: DATABASE EXTENSIONS," IAEA Nuclear Data Section, Vienna, 2008.
- [28] M. Balonov, M. Dubourg, J. G. E. V. Efremenkov, Mishin, R. Rabun, P. Wong and M. Wright, "Management of Waste Containing Tritium and Carbon-14," INTERNATIONAL ATOMIC ENERGY AGENCY, Vienna, 2004.
- [29] N. Rezvani and D. Bolduc, "Monte Carlo Analysis," in *Encyclopedia of Toxicology (Third Edition)*, Academic Press, 2014, pp. 393-396.
- [30] R. Eckhardt, "STAN ULAM, JOHN VON NEUMANN, and the MONTE CARLO METHOD," *Los Alamos Science Special*, vol. 15, pp. 131-143, 1987.
- [31] Atomic Heritage Foundation, "Stanislaw Ulam," Atomic Heritage Foundation, 2022. [Online]. Available: <https://ahf.nuclearmuseum.org/ahf/profile/stanislaw-ulam/>. [Accessed 27 April 2024].
- [32] I. Mickus, "Towards Efficient Monte Carlo," KTH royal institute of technology, Stocholm, 2021.
- [33] J. Leppänen, "Development of a New Monte Carlo Reactor Physics Code," VTT, Helsinki, 2007.

- [34] X-5 Monte Carlo Team, "MCNP - a general monte carlo N-particle transport code, version 5. volume i: Overview and theory," Los Alamos National Laboratory, 2005.
- [35] S. P. Martinson and S. S. Chirayath, "Monte Carlo neutronics benchmarks on nuclear fuel depletion: A review," *Annals of Nuclear Energy*, October 2021.
- [36] Massachusetts Institute of Technology, UChicago Argonne LLC, and OpenMC contributors, "Depletion Chains," OpenMC, 2011-2023. [Online]. Available: <https://openmc.org/%20depletion-chains/>. [Accessed 28 February 2024].
- [37] N. Holden and G. Hedstrom, "ENDF-6 Formats Manual," National Nuclear Data Center, National Nuclear Data Center, 2018.
- [38] M. Chadwick, M. Herma, P. Obložinsky, M. Dunn, Y. Danon, A. Kahler, D. Smith, B. Pritychenko, G. Arbanas, R. Arcilla, R. Brewer, D. Brown, R. Capote, A. Carlson, Y. Cho, H. Derrien, K. Guber, G. Hale and S. H. S. Holloway, "NDF/B-VII.1 Nuclear Data for Science and Technology: Cross Sections, Covariances, Fission Product Yields and Decay Data," *Nuclear Data Sheets*, pp. 2887-2996, December 2011.
- [39] NEA Data Bank Nuclear Data Service team, "Joint Evaluated Fission and Fusion (JEFF) Nuclear Data Library," Nuclear Energy Agency, 22 January 2022. [Online]. Available: <https://www.oecd-nea.org/dbdata/jeff/>. [Accessed 28 February 2024].
- [40] NEA Data Bank participating countries, "JEFF-3.3," Nuclear Energy Agency, 20 November 2017. [Online]. Available: <https://www.oecd-nea.org/dbdata/jeff/jeff33/index.html>. [Accessed 28 February 2024].
- [41] J. Shimwell, "depletion/generate_endf71_chain.py," 22 February 2022. [Online]. Available: https://github.com/openmc-dev/data/blob/master/depletion/generate_endf71_chain.py. [Accessed 28 February 2024].
- [42] L. E. Cevallos-Robalino, R. García-Baonza, G. García-Fernández, E. Gallego and H. R. Vega-Carrillo, "Comparison of FANT results using the ENDF/B-VII.1, JEFF-3.3 and TENDL2017 nuclear data libraries," *Applied Radiation and Isotopes*, vol. Volume 179, 2022.
- [43] B. K. Marjan Kromar, "Comparison of the ENDF/B-VII.0, ENDF/B-VII.1, ENDF/B-VIII.0, and JEFF-3.3 Libraries for the Nuclear Design Calculations of the Nuclear Power Plant Krško With the CORD-2 System," *Journal of Nuclear Engineering and Radiation Science*, p. 5, 2022.
- [44] T. Ware, D. Hanlon, G. Hosking, R. Perry and S. Richards, "Validation of JEFF-3.3 and ENDF/B-VIII.0 nuclear data libraries in ANSWERS codes," in *ND 2019: International Conference on Nuclear Data for Science and Technology*, 2020.
- [45] Openize Pty, "What is an H5 file?," Fileformat, 2024. [Online]. Available: <https://docs.fileformat.com/misc/h5/#what-is-an-h5-file>. [Accessed 28 February 2024].
- [46] Massachusetts Institute of Technology, UChicago Argonne LLC, and OpenMC contributors, "4. Multi-Group Cross Section Library Format," OpenMC, 2011-2024. [Online]. Available: https://docs.openmc.org/en/latest/io_formats/mgxs_library.html. [Accessed 28 February 2024].
- [47] Massachusetts Institute of Technology, UChicago Argonne LLC, and OpenMC contributors, "2. Depletion Chain - chain.xml," OpenMC, 2011-2023. [Online]. Available: https://docs.openmc.org/en/stable/io_formats/depletion_chain.html. [Accessed 7 May 2024].
- [48] Massachusetts Institute of Technology, UChicago Argonne LLC, and OpenMC contributors, "openmc.Material," OpenMC, 2011-2024. [Online]. Available: <https://docs.openmc.org/en/latest/pythonapi/generated/openmc.Material.html>. [Accessed 16 April 2024].

- [49] K. Tonoike, H. Sono, M. Umeda, Y. Yamane, T. Kugo and K. Suyama, "Options of Principles of Fuel Debris Criticality Control in Fukushima Daiichi Reactors," in *Nuclear Back-end and Transmutation Technology for Waste Disposal Beyond the Fukushima Accident*, Osaka, Kyoto University, 2015, pp. 251-259.
- [50] Massachusetts Institute of Technology, UChicago Argonne LLC, and OpenMC contributors, "openmc.deplete – Depletion," OpenMC, 2011-2024. [Online]. Available: <https://docs.openmc.org/en/latest/pythonapi/deplete.html>. [Accessed 16 April 2024].
- [51] Massachusetts Institute of Technology, UChicago Argonne LLC, and OpenMC contributors, "openmc.deplete.StepResult¶," OpenMC, 2011-2024. [Online]. Available: <https://docs.openmc.org/en/latest/pythonapi/generated/openmc.deplete.StepResult.html>. [Accessed 7 May 2024].
- [52] Massachusetts Institute of Technology, UChicago Argonne LLC, and OpenMC contributors, "Source code for openmc.deplete.stepsresult," OpenMC, 2011-2024. [Online]. Available: https://docs.openmc.org/en/latest/_modules/openmc/deplete/stepsresult.html#StepResult. [Accessed 7 May 2024].
- [53] R. J. Amdur and E. L. Mazzaferri, "Half-Life and Emission Products of I-131," in *Essentials of thyroid cancer mangment*, Boston, Springer, Boston, MA, 2005, p. 165–168.
- [54] Kaasaegse Tuumaenergia Infokeskus, "Tuumküttus," Kaasaegse Tuumaenergia Infokeskus, 2024. [Online]. Available: <https://moodulreaktor.ee/tuumkutus/>. [Accessed 05 03 2024].
- [55] N. M. Ghoniem and Y. Cui, "1.22 - Dislocation Dynamics Simulations of Defects in Irradiated Materials," in *Comprehensive Nuclear Materials(Second Edition)*, Los Angele, University of California, 2020, pp. 689-716.

9 Appendix

9.1 Appendix 1. Depletion file creation modified code

```
%matplotlib inline
import argparse
import tarfile
import sys
import os
from pathlib import Path
from shutil import rmtree
from urllib.parse import urljoin

import openmc.data
import urllib.request

from zipfile import ZipFile

import openmc.deplete

def main():
    endf_dir = os.environ.get("OPENMC_ENDF_DATA")
    if endf_dir is not None:
        endf_dir = Path(endf_dir)

    decay_files = list((endf_dir / "decay").glob("*ASC"))
    neutron_files = list((endf_dir / "neutron").glob("*jeff33"))
    fpy_files = list((endf_dir / "fission").glob("*ASC"))

    # Remove erroneous Be7 evaluation that can cause problems
    #decay_files.remove(endf_dir / "decay" / "dec-004_Be_007.endf")
    #neutron_files.remove(endf_dir / "neutrons" / "n-004_Be_007.endf")

    # check files exist
    for flist, ftype in [(decay_files, "Radioactive decay data"), (neutron_files, "neutron"), (fpy_files, "fpy")]:
        if not flist:
            raise IOError("No {} endf files found in {}".format(ftype, endf_dir))

    chain = openmc.deplete.Chain.from_endf(decay_files, fpy_files, neutron_files)
    chain.export_to_xml('chain_jeff3.3.xml')

if __name__ == '__main__':
    main()
```

9.2 Appendix 2. Fission yields file formatting code

```
import sys
import os
import numpy as np
import pandas as pd
f = open("JEFF33-nfy.asc", 'r')
print(f)
lines=f.readlines()
file = open('./myfile.txt', 'w')
file.write('                                0 0 0 0\n')
i=1
j=0
k=0
nimi=' '
for line in lines:
    l=line.split(' ')
    if i == 5:
        if l[1]== '92-U':
            nimi=str(l[1]+l[2]+'.ASC')
        elif l[1]== '95-Am-242MSEL':
            nimi=('95-Am-242.ASC')
        else:
            nimi=str(l[1]+'.ASC')
    a=lines[k-1].split(' ')
    if lines[k]!= lines[-1]:
        if l[-1]=='\n' and a[-1]=='\n':
            file.write(line)
            os.rename('./myfile.txt', nimi)
            file.close()
            file = open('./myfile.txt', 'w')
            i=0
        else:
            file.write(line)
            os.rename('./myfile.txt', nimi)
            file=open(nimi, 'a')
            file.write(line)

    k=k+1
    i=i+1
```

```
for filename in os.listdir('/Users/eliisekaha/Documents/nfy'):
    if filename.endswith(".ASC"):
        f = open(filename, 'a')
        if filename=='96-Cm-245.ASC':
            f.write('\n                                0 0 0 0\n')
            f.write(' 0.0000E+00 0.0000E+00          0          0          0          0 -1 0 0 0\n')
            f.close()
```

9.3 Appendix 3. Material definition formatting example

```
uo2_49 = openmc.Material(name="uo2 4.9% enrichment")
uo2_49.add_nuclide('U234', 8.5649e-6, percent_type='ao')
uo2_49.add_nuclide('U235', 1.1221e-3, percent_type='ao')
uo2_49.add_nuclide('U238', 2.1495e-2, percent_type='ao')
uo2_49.add_nuclide('O16', 4.5252e-2, percent_type='ao')
```

9.4 Appendix 4. Volume data extraction code example

```
results_VIII_40 = openmc.deplete.Results("/root/VIII/depletion_results_VII.1_40%.h5")

nuclide_names = ["U234", "U235", "U236", "U238", "Np237", "Pu238", "Pu239", "Pu240", "Pu241", "Pu242", "Am241", "Am243", "Cm244",
                 "Sr90", "Mo95", "Tc99", "Ru101", "Rh103", "Ag109", "I129", "Xe131", "Cs133", "Cs134", "Cs137", "Ce144", "Nd143",
                 "Nd145", "Nd148", "Sm147", "Sm149", "Sm150", "Sm151", "Sm152", "Eu153", "Eu154", "Eu155", "Gd155", "Gd156", "Gd157", "Gd158"]

stepresult = results[-1]
AtomsDict_VIII_40 = {}
total_volume = 0
for idd, midx in stepresult.index_mat.items():
    volume = stepresult.volume[idd]
    if "U238" in stepresult.index_nuc.keys():
        total_volume += volume
    for nuc, nidx in stepresult.index_nuc.items():
        if nuc in nuclide_names:
            atoms = stepresult.data[0][int(midx)][int(nidx)]
            if nuc in AtomsDict_VIII_40:
                AtomsDict_VIII_40[nuc] += atoms
            else:
                AtomsDict_VIII_40[nuc] = atoms

for key, value in AtomsDict_VIII_40.items():
    AtomsDict_VIII_40[key] = value / (total_volume * 1e24) # 1e24/cm3

print(AtomsDict_VIII_40)
```

9.5 Appendix 5. Phase III-C benchmark results for 40% void

Table 3.12(3). All results for Case 11b (40% void, 50 GWd/tHM, 5-year cooling) actinides and fission products [$10^{24}/\text{cm}^3$] reported by participants

	c	d	e	f	g	h	i	Average	2 σ	2 $\sigma^{(i)}$
²³⁴ U	3.58E-06	3.58E-06	3.50E-06	3.54E-06	3.05E-06	3.73E-06	3.57E-06	3.55E-06	2.66E-07	7.48E-02
²³⁸ U	1.15E-04	1.15E-04	1.08E-04	1.15E-04	1.11E-04	1.14E-04	1.17E-04	1.15E-04	7.21E-06	6.28E-02
²³⁶ U	1.24E-04	1.24E-04	1.24E-04	1.24E-04	1.24E-04	1.23E-04	1.19E-04	1.23E-04	3.78E-06	3.07E-02
²³⁸ U	2.07E-02	1.83E-05	8.81E-04							
²³⁷ Np	1.32E-05	1.30E-05	1.33E-05	1.28E-05	1.31E-05	1.26E-05	1.23E-05	1.29E-05	8.75E-07	6.77E-02
²³⁸ Pu	6.12E-06	6.04E-06	6.60E-06	5.50E-06	6.00E-06	6.98E-06	5.87E-06	6.29E-06	8.77E-07	1.39E-01
²³⁹ Pu	1.02E-04	1.01E-04	9.87E-05	9.94E-05	9.79E-05	9.66E-05	9.79E-05	9.78E-05	5.94E-06	6.07E-02
²⁴⁰ Pu	6.44E-05	6.47E-05	6.36E-05	6.28E-05	6.25E-05	6.12E-05	6.16E-05	6.24E-05	3.20E-06	5.14E-02
²⁴¹ Pu	2.30E-05	2.28E-05	2.23E-05	2.24E-05	2.21E-05	2.20E-05	2.26E-05	2.24E-05	1.16E-06	5.17E-02
²⁴² Pu	2.04E-05	2.04E-05	2.12E-05	2.01E-05	2.03E-05	2.05E-05	2.01E-05	2.04E-05	9.59E-07	4.71E-02
²⁴¹ Am	7.61E-06	7.54E-06	7.18E-06	7.42E-06	7.15E-06	7.12E-06	7.46E-06	7.33E-06	4.62E-07	6.31E-02
²⁴³ Am	4.99E-06	4.95E-06	4.74E-06	4.73E-06	4.31E-06	4.35E-06	4.32E-06	4.64E-06	5.61E-07	1.21E-01
²⁴⁴ Cm	1.71E-06	1.69E-06	1.65E-06	1.65E-06	1.50E-06	1.66E-06	1.49E-06	1.63E-06	1.69E-07	1.04E-01
⁹⁰ Sr	4.00E-05	4.01E-05	3.96E-05	4.00E-05	3.99E-05	4.00E-05	4.07E-05	4.00E-05	6.86E-07	1.72E-02
⁹⁵ Mo	6.20E-05	6.20E-05	6.29E-05	6.17E-05	6.15E-05	6.20E-05	6.19E-05	6.19E-05	7.21E-07	1.16E-02
⁹⁹ Tc	6.22E-05	6.23E-05	6.25E-05	6.21E-05	6.03E-05	6.22E-05	6.25E-05	6.20E-05	1.84E-06	2.96E-02
¹⁰¹ Ru	6.14E-05	6.14E-05	6.25E-05	6.09E-05	6.04E-05	6.11E-05	6.01E-05	6.11E-05	1.09E-06	1.78E-02
¹⁰³ Rh	3.30E-05	3.29E-05	3.27E-05	3.16E-05	3.06E-05	3.27E-05	3.15E-05	3.23E-05	1.07E-06	3.32E-02
¹⁰⁹ Ag	5.81E-06	5.78E-06	6.29E-06	4.05E-06	5.19E-06	5.62E-06	6.38E-06	5.42E-06	1.40E-06	2.58E-01
¹²⁹ I	9.55E-06	9.54E-06	1.06E-05	8.67E-06	8.89E-06	8.99E-06	1.04E-05	9.49E-06	1.61E-06	1.70E-01
¹³¹ Xe	2.40E-05	2.40E-05	2.37E-05	2.24E-05	2.37E-05	2.33E-05	2.36E-05	2.34E-05	1.41E-06	6.03E-02
¹³³ Cs	6.54E-05	6.55E-05	6.48E-05	6.51E-05	6.40E-05	6.47E-05	6.54E-05	6.49E-05	1.64E-06	2.52E-02
¹³⁴ Cs	1.39E-06	1.37E-06	1.42E-06	1.37E-06	1.36E-06	1.39E-06	1.31E-06	1.38E-06	1.15E-07	8.34E-02
¹³⁷ Cs	6.19E-05	6.19E-05	6.23E-05	6.17E-05	6.16E-05	6.14E-05	6.25E-05	6.16E-05	1.17E-06	1.89E-02
¹⁴⁴ Ce	1.26E-07	1.26E-07	1.26E-07	1.25E-07	1.24E-07	1.25E-07	1.26E-07	1.25E-07	1.88E-09	1.51E-02
¹⁴³ Nd	3.62E-05	3.61E-05	3.52E-05	3.60E-05	3.52E-05	3.58E-05	3.60E-05	3.59E-05	7.77E-07	2.17E-02

Table 3.14(2). All results for Case 12b (70% void, 50 GWd/tHM, 5-year cooling) actinides and fission products [$10^{24}/\text{cm}^3$] reported by participants (continued)

¹⁴⁵ Nd	3.47E-05	3.45E-05	3.46E-05	3.54E-05	3.53E-05	3.51E-05	3.46E-05	3.41E-05	3.43E-05	3.47E-05	3.52E-05	3.53E-05	3.44E-05	3.52E-05
¹⁴⁸ Nd	1.97E-05	1.99E-05	1.99E-05	2.01E-05	2.01E-05	1.98E-05	1.98E-05	1.98E-05	2.00E-05	1.99E-05	1.98E-05	2.01E-05	1.99E-05	2.01E-05
¹⁴⁷ Sm	1.05E-05	1.06E-05	1.04E-05	1.05E-05	9.67E-06	9.55E-06	9.30E-06	9.96E-06	1.06E-05	1.06E-05	9.62E-06	9.68E-06	1.04E-05	1.06E-05
¹⁴⁹ Sm	1.11E-07	1.06E-07	1.07E-07	1.08E-07	1.18E-07	1.17E-07	1.27E-07	1.04E-07	1.00E-07	9.99E-08	1.17E-07	1.17E-07	1.06E-07	1.12E-07
¹⁵⁰ Sm	1.46E-05	1.49E-05	1.50E-05	1.55E-05	1.46E-05	1.45E-05	1.45E-05	1.47E-05	1.43E-05	1.44E-05	1.45E-05	1.46E-05	1.50E-05	1.55E-05
¹⁵¹ Sm	5.01E-07	4.54E-07	4.65E-07	4.80E-07	5.72E-07	5.60E-07	5.92E-07	4.50E-07	4.55E-07	4.47E-07	5.67E-07	5.68E-07	4.51E-07	4.80E-07
¹⁵² Sm	5.27E-06	4.81E-06	4.79E-06	4.96E-06	5.96E-06	5.89E-06	5.92E-06	4.88E-06	4.85E-06	4.80E-06	5.92E-06	5.97E-06	4.78E-06	4.95E-06
¹⁵³ Eu	6.23E-06	6.05E-06	6.05E-06	6.15E-06	6.53E-06	6.32E-06	6.49E-06	5.67E-06	6.14E-06	6.11E-06	6.32E-06	6.53E-06	6.02E-06	6.30E-06
¹⁵⁴ Eu	9.19E-07	9.15E-07	9.06E-07	7.87E-07	9.25E-07	9.36E-07	8.86E-07	8.44E-07	9.14E-07	9.12E-07	9.40E-07	9.22E-07	9.13E-07	1.54E-06
¹⁵⁵ Eu	1.54E-07	2.15E-07	2.14E-07	2.18E-07	1.62E-07	1.60E-07	2.42E-07	1.97E-07	2.23E-07	2.23E-07	1.54E-07	1.62E-07	2.15E-07	2.26E-07
¹⁵⁵ Gd	2.31E-08	2.54E-07	2.57E-07	2.63E-07	1.92E-07	1.88E-07	3.00E-07	2.38E-07	2.52E-07	2.56E-07	1.96E-07	1.93E-07	2.57E-07	2.59E-07
¹⁵⁶ Gd	9.07E-05	9.74E-05	9.68E-05	9.77E-05	9.87E-05	9.80E-05	9.69E-05	9.75E-05	9.68E-05	9.62E-05	9.81E-05	9.89E-05	9.67E-05	9.69E-05
¹⁵⁷ Gd	2.64E-08	2.81E-08	3.26E-08	3.05E-08	2.82E-08	2.84E-08	3.85E-08	2.79E-08	3.12E-08	3.96E-08	2.86E-08	2.78E-08	3.11E-08	3.09E-08
¹⁵⁸ Gd	1.09E-04	1.14E-04	1.15E-04	1.14E-04	1.14E-04	1.15E-04	1.15E-04	1.15E-04	1.15E-04	1.15E-04	1.15E-04	1.14E-04	1.15E-04	1.14E-04

9.6 Appendix 6. Phase III-C benchmark results for 70% void

Table 3.14(3). All results for Case 12b (70% void, 50 GWd/tHM, 5-year cooling) actinides and fission products [$10^{24}/\text{cm}^3$] reported by participants

	c	d	e	f	g	h	i	Average	2*σ	2*σ ^(f)
²³⁴ U	3.56E-06	3.56E-06	3.48E-06	3.53E-06	3.03E-06	3.71E-06	3.54E-06	3.53E-06	2.86E-07	8.10E-02
²³⁵ U	1.46E-04	1.45E-04	1.38E-04	1.45E-04	1.40E-04	1.43E-04	1.47E-04	1.45E-04	8.64E-06	5.98E-02
²³⁶ U	1.24E-04	1.25E-04	1.24E-04	1.25E-04	1.24E-04	1.23E-04	1.19E-04	1.24E-04	4.44E-06	3.59E-02
²³⁸ U	2.06E-02	2.07E-02	2.06E-02	2.07E-02	2.07E-02	2.07E-02	2.07E-02	2.07E-02	1.85E-05	8.95E-04
²³⁷ Np	1.46E-05	1.43E-05	1.47E-05	1.39E-05	1.44E-05	1.38E-05	1.35E-05	1.42E-05	1.27E-06	8.90E-02
²³⁸ Pu	7.38E-06	7.27E-06	7.91E-06	6.60E-06	7.21E-06	8.18E-06	7.05E-06	7.53E-06	1.02E-06	1.36E-01
²³⁹ Pu	1.30E-04	1.28E-04	1.25E-04	1.25E-04	1.23E-04	1.21E-04	1.24E-04	1.24E-04	8.80E-06	7.11E-02
²⁴⁰ Pu	7.03E-05	7.06E-05	6.95E-05	6.91E-05	6.84E-05	6.66E-05	6.71E-05	6.80E-05	3.86E-06	5.68E-02
²⁴¹ Pu	2.80E-05	2.75E-05	2.69E-05	2.69E-05	2.65E-05	2.64E-05	2.73E-05	2.70E-05	1.87E-06	6.92E-02
²⁴² Pu	1.93E-05	1.92E-05	2.01E-05	1.90E-05	1.93E-05	1.96E-05	1.91E-05	1.94E-05	1.05E-06	5.41E-02
²⁴¹ Am	9.37E-06	9.19E-06	8.78E-06	8.99E-06	8.68E-06	8.65E-06	9.12E-06	8.95E-06	6.97E-07	7.78E-02
²⁴³ Am	5.33E-06	5.27E-06	5.08E-06	4.95E-06	4.55E-06	4.63E-06	4.64E-06	4.95E-06	5.91E-07	1.19E-01
²⁴⁴ Cm	2.05E-06	2.02E-06	1.99E-06	1.95E-06	1.78E-06	1.99E-06	1.81E-06	1.97E-06	1.97E-07	1.00E-01
⁹⁰ Sr	3.91E-05	3.92E-05	3.87E-05	3.91E-05	3.90E-05	3.91E-05	3.98E-05	3.91E-05	7.21E-07	1.84E-02
⁹⁹ Mo	6.10E-05	6.11E-05	6.20E-05	6.08E-05	6.07E-05	6.12E-05	6.10E-05	6.11E-05	7.79E-07	1.28E-02
⁹⁹ Tc	6.16E-05	6.18E-05	6.21E-05	6.15E-05	5.96E-05	6.19E-05	6.21E-05	6.15E-05	1.95E-06	3.17E-02
¹⁰¹ Ru	6.09E-05	6.09E-05	6.22E-05	6.04E-05	6.01E-05	6.07E-05	5.97E-05	6.08E-05	1.12E-06	1.85E-02
¹⁰³ Rh	3.37E-05	3.35E-05	3.32E-05	3.22E-05	3.12E-05	3.31E-05	3.21E-05	3.29E-05	1.10E-06	3.33E-02
¹⁰⁹ Ag	5.98E-06	5.94E-06	6.44E-06	4.20E-06	5.33E-06	5.79E-06	6.57E-06	5.57E-06	1.39E-06	2.49E-01
¹²⁹ I	9.81E-06	9.79E-06	1.08E-05	8.90E-06	9.14E-06	9.22E-06	1.06E-05	9.73E-06	1.64E-06	1.68E-01
¹³¹ Xe	2.37E-05	2.36E-05	2.33E-05	2.17E-05	2.34E-05	2.30E-05	2.32E-05	2.30E-05	1.67E-06	7.26E-02
¹³³ Cs	6.46E-05	6.48E-05	6.41E-05	6.44E-05	6.34E-05	6.41E-05	6.47E-05	6.42E-05	1.75E-06	2.73E-02
¹³⁴ Cs	1.47E-06	1.44E-06	1.50E-06	1.43E-06	1.43E-06	1.46E-06	1.38E-06	1.46E-06	1.35E-07	9.23E-02
¹³⁷ Cs	6.18E-05	6.18E-05	6.22E-05	6.15E-05	6.16E-05	6.14E-05	6.25E-05	6.16E-05	1.20E-06	1.95E-02
¹⁴⁴ Ce	1.25E-07	1.25E-07	1.26E-07	1.24E-07	1.24E-07	1.25E-07	1.25E-07	1.24E-07	1.84E-09	1.48E-02
¹⁴³ Nd	3.90E-05	3.88E-05	3.81E-05	3.87E-05	3.80E-05	3.85E-05	3.87E-05	3.86E-05	7.84E-07	2.03E-02

Table 3.14(3). All results for Case 12b (70% void, 50 GWd/tHM, 5-year cooling) actinides and fission products [$10^{24}/\text{cm}^3$] reported by participants (continued)

¹⁴⁵ Nd	3.45E-05	3.46E-05	3.55E-05	3.42E-05	3.38E-05	3.49E-05	3.54E-05	3.48E-05	8.25E-07	2.37E-02
¹⁴⁸ Nd	1.99E-05	1.99E-05	2.03E-05	1.99E-05	1.99E-05	1.97E-05	1.99E-05	1.99E-05	2.87E-07	1.44E-02
¹⁴⁷ Sm	1.05E-05	1.06E-05	1.05E-05	1.05E-05	8.27E-06	1.07E-05	1.06E-05	1.03E-05	1.00E-06	9.75E-02
¹⁴⁹ Sm	1.04E-07	1.03E-07	9.52E-08	1.07E-07	8.92E-08	1.04E-07	1.07E-07	1.06E-07	1.51E-08	1.43E-01
¹⁵⁰ Sm	1.51E-05	1.51E-05	1.42E-05	1.48E-05	1.40E-05	1.49E-05	1.50E-05	1.47E-05	9.41E-07	6.39E-02
¹⁵¹ Sm	4.65E-07	4.60E-07	4.46E-07	4.65E-07	4.25E-07	4.36E-07	4.66E-07	4.76E-07	9.02E-08	1.89E-01
¹⁵² Sm	4.89E-06	4.83E-06	4.83E-06	4.76E-06	4.70E-06	4.78E-06	5.10E-06	5.05E-06	9.64E-07	1.91E-01
¹⁵³ Eu	6.10E-06	6.10E-06	6.08E-06	6.04E-06	5.51E-06	5.98E-06	6.01E-06	6.10E-06	4.24E-07	6.95E-02
¹⁵⁴ Eu	9.33E-07	9.29E-07	9.14E-07	9.11E-07	8.30E-07	8.79E-07	7.82E-07	9.12E-07	2.36E-07	2.59E-01
¹⁵⁵ Eu	2.22E-07	2.17E-07	2.14E-07	2.13E-07	1.97E-07	2.08E-07	2.09E-07	2.05E-07	4.69E-08	2.29E-01
¹⁵⁵ Gd	2.66E-07	2.59E-07	2.58E-07	2.56E-07	2.42E-07	2.53E-07	2.52E-07	2.41E-07	9.09E-08	3.77E-01
¹⁵⁶ Gd	9.78E-05	9.68E-05	9.77E-05	9.12E-05	9.66E-05	9.70E-05	9.57E-05	9.69E-05	3.32E-06	3.42E-02
¹⁵⁷ Gd	2.89E-08	2.94E-08	2.80E-08	3.05E-08	3.00E-08	3.12E-08	3.54E-08	3.10E-08	7.75E-09	2.50E-01
¹⁵⁸ Gd	1.14E-04	1.14E-04	1.14E-04	1.14E-04	1.15E-04	1.14E-04	1.16E-04	1.14E-04	2.01E-06	1.76E-02

9.7 Appendix 7. Mass data extraction code example

```
#results = openmc.deplete.Results("/root/VIII/depletion_results_VII.1_0%.h5")
#results = openmc.deplete.Results("/root/VIII/depletion_results_VII.1_40%.h5")
#results = openmc.deplete.Results("/root/VIII/depletion_results_VII.1_70%.h5")
#results = openmc.deplete.Results("/root/JEFF33/depletion_results-JEFF3_0%.h5")
#results = openmc.deplete.Results("/root/JEFF33/depletion_results-JEFF3_40%.h5")
#results = openmc.deplete.Results("/root/JEFF33/depletion_results-JEFF3_70%.h5")
#results= openmc.deplete.Results("/root/VIII0/depletion_results_VIII.0_0%.h5")
#results= openmc.deplete.Results("/root/VIII0/depletion_results_VIII.0_40%.h5")
results= openmc.deplete.Results("/root/VIII0/depletion_results_VIII.0_70%.h5")

power_density = 25.3 # MW/gHM
stepresult = results[-1]
MassDict= {}
for idd in stepresult.index_mat.items():
    if "U238" in stepresult.index_nuc.keys():
        times, mass = results.get_mass(str(idd[0]), "I129", mass_units="g", time_units="d")
        print(times)
        for i in range(len(times)):
            burnup = times[i] * power_density/ 1000
            if burnup in MassDict :
                MassDict[burnup] += mass[i]/1000
            else:
                MassDict[burnup] = mass[i]/1000
```

9.8 Appendix 8. Source term STEP-3 fuel assembly

Table 1: STEP-3 fuel assembly source term

Volatile gases	Burn-up [GWd/tU]			Approximation	
	5	25	50	Linear	Quadratic
	Radioactivity [Bq]				
C-14	13790.6265	78075.3319	167850.5378	$3311x - 3212$	$9.7x^2 + 2896x - 681$
H-3	447387983.6482	2335702407.7515	4871874809.0195	$9.64 \cdot 10^7 x - 4.58 \cdot 10^7$	$1.65 \cdot 10^5 x^2 + 8.94 \cdot 10^7 x - 2.81 \cdot 10^6$
Kr-85	12701833618.1246	53214165770.7036	85229817085.9810	$1.81 \cdot 10^9 x + 4.78 \cdot 10^9$	$-1.73 \cdot 10^7 \cdot x^2 + 2.55 \cdot 10^9 \cdot x + 2.67 \cdot 10^8$
I-129	17516.3649	105196.5389	228501.9801	$4533x - 5792$	$15.95x^2 + 3851x - 1631$
I-131	11017057379.1577	117424610.4661	12216574507.4527		

9.9 Appendix 9. Non-exclusive licence for reproduction and publication of a graduation thesis

Annex
to Rector's directive No 1-8/17 of 7 April 2020

Non-exclusive licence for reproduction and publication of a graduation thesis³

I _____ Eliise Kaha _____ (author's name)

1. grant Tallinn University of Technology free licence (non-exclusive licence) for my thesis
_____ Estimating the inventory of volatile gases in a BWR reactor using OpenMC _____,
(title of the graduation thesis)

supervised by _____ Marti Jeltsov, Hando Tohver _____,
(supervisor's name)

1.1 to be reproduced for the purposes of preservation and electronic publication of the graduation thesis, incl. to be entered in the digital collection of the library of Tallinn University of Technology until expiry of the term of copyright;

1.2 to be published via the web of Tallinn University of Technology, incl. to be entered in the digital collection of the library of Tallinn University of Technology until expiry of the term of copyright.

2. I am aware that the author also retains the rights specified in clause 1 of the non-exclusive licence.

3. I confirm that granting the non-exclusive licence does not infringe other persons' intellectual property rights, the rights arising from the Personal Data Protection Act or rights arising from other legislation.

_____ 20.05.2024 _____ (date)

³ The non-exclusive licence is not valid during the validity of access restriction indicated in the student's application for restriction on access to the graduation thesis that has been signed by the school's dean, except in case of the university's right to reproduce the thesis for preservation purposes only. If a graduation thesis is based on the joint creative activity of two or more persons and the co-author(s) has/have not granted, by the set deadline, the student defending his/her graduation thesis consent to reproduce and publish the graduation thesis in compliance with clauses 1.1 and 1.2 of the non-exclusive licence, the non-exclusive license shall not be valid for the period.